PRINCIPLES AND PRACTICE OF COHERENT X-RAY DIFFRACTION IMAGING

Malcolm Howells, Stefano Marchesini, Janos Kirz, David Shapiro	*Lawrence Berkeley National Laboratory*
John Spence, Uwe Weierstall	*Arizona State University*
Henry Chapman, Anton Barty, Stefan Hau-Riege, Alex Noy	*Lawrence Livermore National Laboratory*
Chris Jacobsen, Huijie Miao, Aaron Neiman, David Sayre, Janos Kirz	*Stony Brook University*
Enju Lima, Lutz Wiegart, Malcolm Howells, Anders Madsen, Petra Pernot, Federico Zontone	*European Synchrotron Radiation Facility*

LENSLESS COHERENT X-RAY DIFFRACTION IMAGING (CXDI)

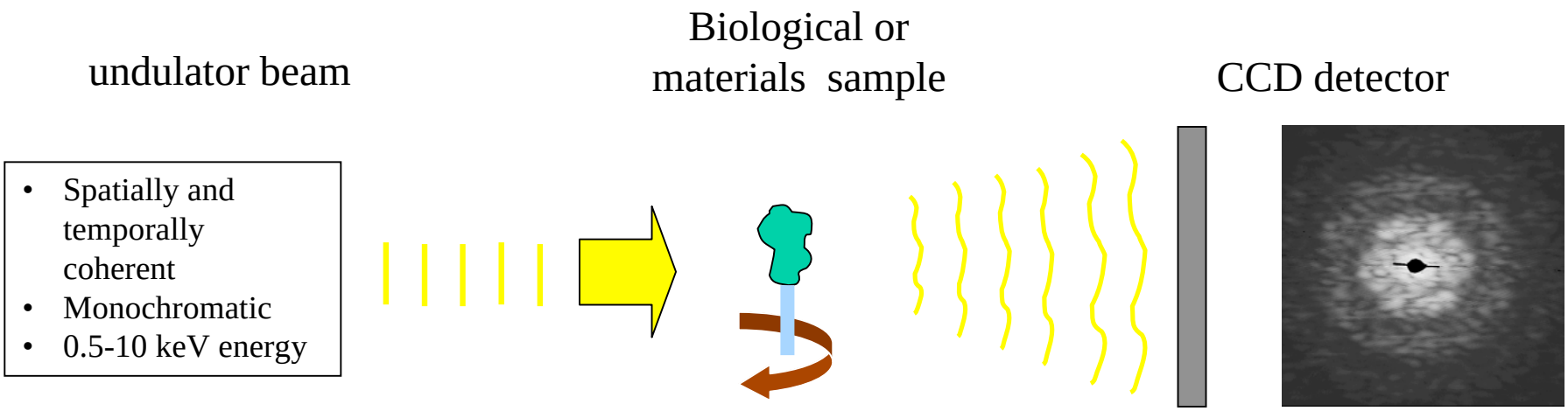

- To get a 2D image:
  - Record one diffraction pattern which gives Fourier amplitudes
  - Use a 2D phase retrieval algorithm to get their phases
  - Get an image by Fourier inversion
- To get a 3D image:
  - Record a tilt series of diffraction patterns
  - Insert the resulting Fourier amplitudes into a 3D Fourier space
  - Use a 3D phase retrieval algorithm to get their phases
  - Get an image by Fourier inversion ("true" 3D)
- True 3D is required when the collection angle includes a significantly curved portion of the Ewald sphere or when low-dose imaging is required

WHY IS "LENSLESS" ATTRACTIVE?

- Zone-plate lenses waste x-rays which also hurts resolution when the imaging is damage limited
- For example with 20 nm zone plates at the oxygen edge energy, we have 8x loss for diffraction efficiency, 2x loss for window transmission, 5x loss for modulation transfer function (MTF) at 15 nm feature size (graph below)
- Zone plates
  - are hard to make with good resolution
  - may have very short focal length (<1mm) which makes sample rotation hard
  - may have a depth of field less than the sample thickness → the image is not a projection
- Nevertheless zone-plate microscopes work and have many advantages and are viewed as complementary to diffractive imaging

(MTF=modulation transfer function)

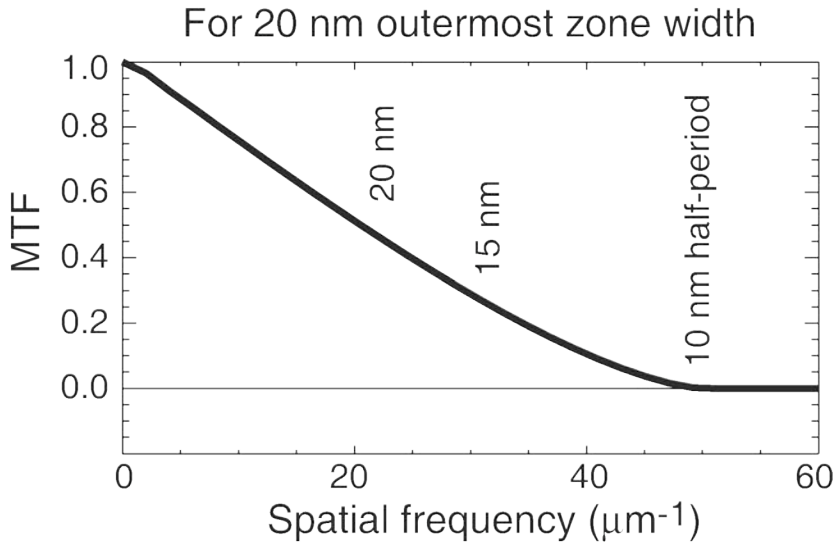

Slide: C. Jacobsen, Stony Brook

WHERE DOES CXDM FIT IN WITH OTHER 3D MICROSCOPES TODAY?

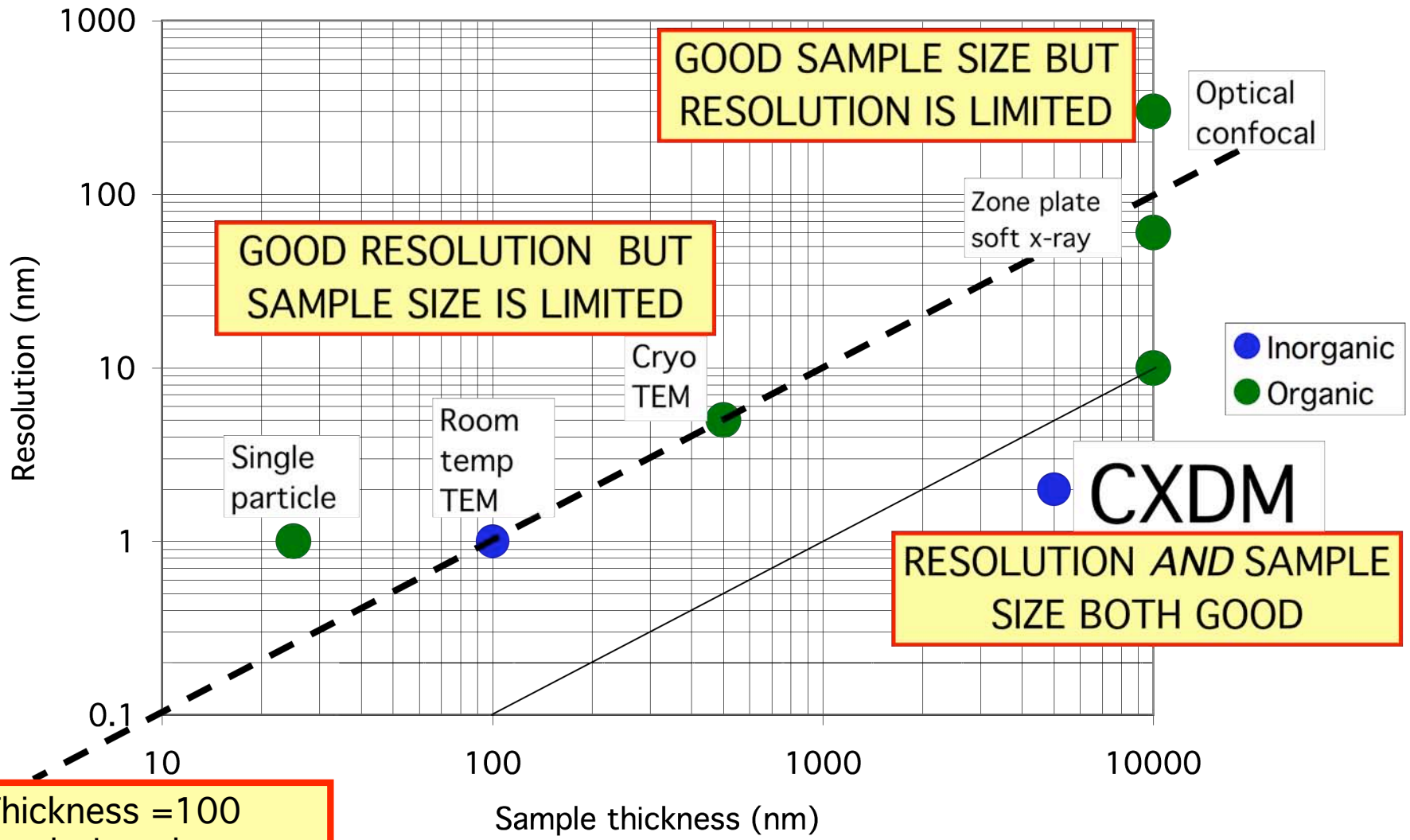

COHERENT X-RAY DIFFRACTION IMAGING: HISTORY

Sayre (1952) - Fundamentals of sampling the wave amplitude and wave intensity

Gerchberg and Saxton (1972) - First phase-retrieval algorithm successful on test data

Sayre (1980) - Idea to do "crystallography" with non-periodic objects (i. e. attempt phase retrieval) and exploit the cross-section advantage of soft x-rays

Sayre, Yun, Chapman, Miao, Kirz (1980's and 1990's) - development of the experimental technique

Fienup (1978-) - Development of practical phase-retrieval algorithms including use of the combination of support constraint and oversampling of the amplitude pattern

Miao, Charalambous, Kirz and Sayre (1999) - first demonstration of 2-D CXDM using a Fienup-style algorithm at 0.73 keV x-ray energy, 75 nm resolution

Miao et al (2000) - imaging of a fixed biological sample in 2-D at 30 nm resolution

Miao et al (2001) - improved resolution in 2-D: 7 nm
achievement of 3-D with moderate resolution: 55 nm

Robinson et al (2001-3) - Application to microcrystals and defects - 3D reconstruction - hardest x-rays

ALS group 2002-5 - reconstruction without use of other micoscopes - 3D reconstructions with many (up to 280) views and 10 nm resolution

ROOTS OF CXDI WERE IN THE US BUT IT IS NOW SPREADING MORE WIDELY

"Old" programs (>5years):

- Brookhaven/Stony Brook
  - Original concept and first experimental demonstration in 1999
  - Developed cryo CXDI for bio-samples
  - Now combined with the Berkeley/Livermore/Arizona-State effort at ALS
- UCLA/SSRL
  - User experiments at SPring8, 2D and 3D reconstructions
  - Resolution record 7 nm
- Advanced Photon Source
  - Dedicated hard x-ray beam line developed by University of Illinois
  - Microcrystal studies, 3D reconstructions
- Advanced Light Source: Arizona State, Lawrence Berkeley Lab, Lawrence Livermore Lab
  –3D with large numbers of views (up to 280) and 10 nm resolution

Newer programs:

- SPring 8 – local program
- Swiss Light Source
  - New phasing methods
- BESSY
  - Holographic methods
- XFELs – DESY, LCLS
  - Damage-avoidance experiments
- ESRF
  - TROICA beam line - continuing development of cryo CXDI for bio-samples

3D IMAGE OF A MATERIALS-SCIENCE SAMPLE USING CXDI (UCLA GROUP)

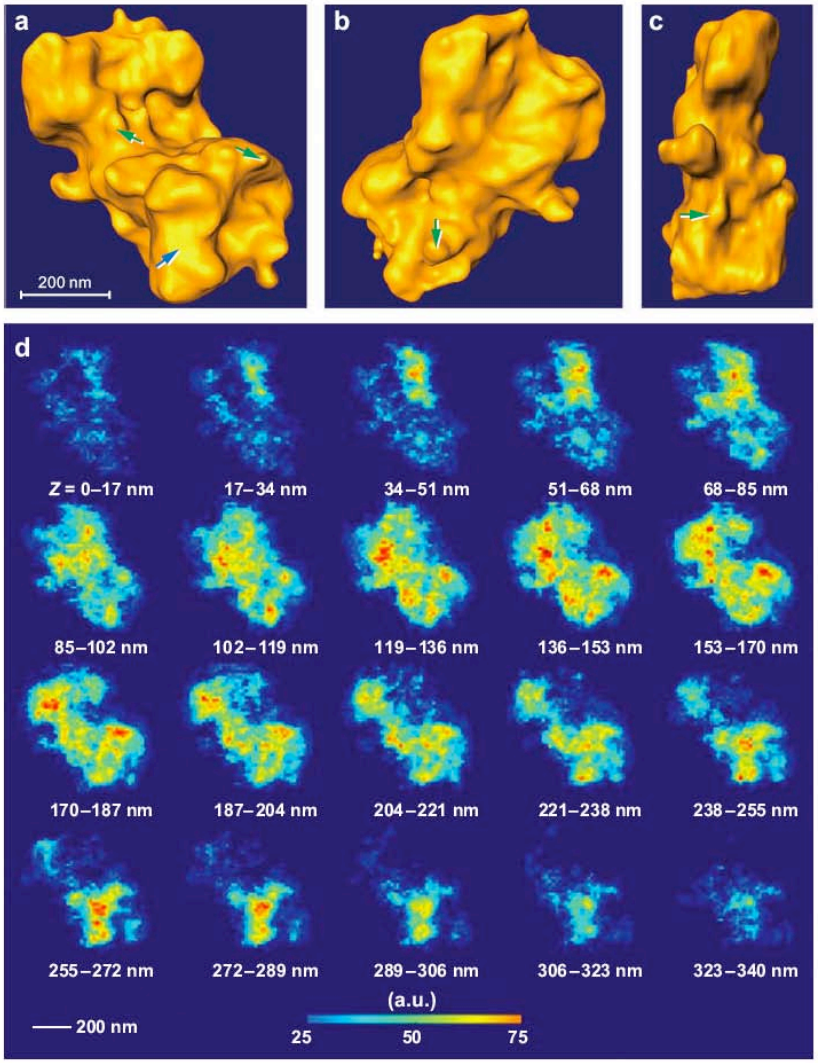

[Miao et al PRL 215503 (2006)]

- Surface rendering and through focus series of a reconstructed 3D GaN "quantum dot" particle
- Resolution 17 nm

a) The front surface

b) The back surface

c) The side surface

d) The 3D internal structure showing regions of low electron density (blue) corresponding to β-Ga_2O_3 and of high density corresponding to GaN cores

APPLICATION TO IMAGING NANOCRYSTALS

Robinson et al PRL, **87**, 195505 (2001), Williams et al PRL, **90**, 175501 (2003)

111 Bragg spot of 2 μm Au crystal

Diffraction pattern around the spot (sampled at 30 planes)

Views of the reconstructed image at nine depth values

SEM of nanocrystal

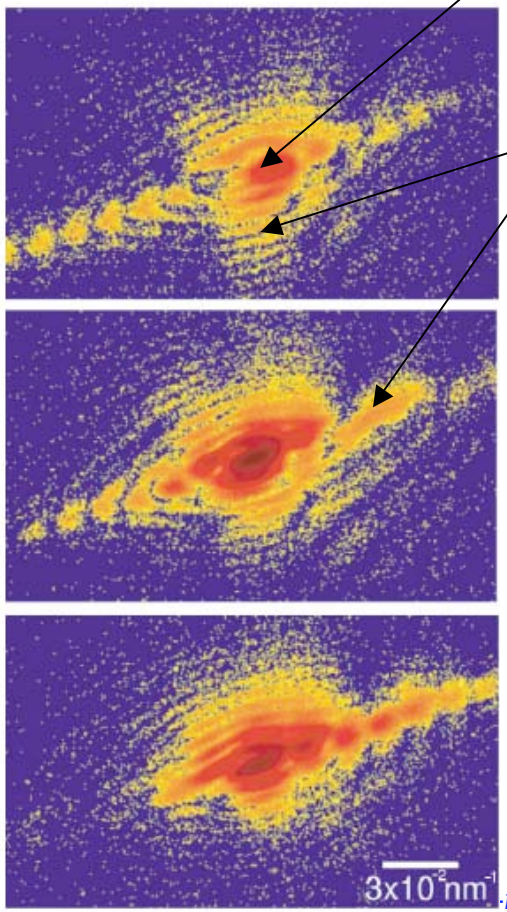

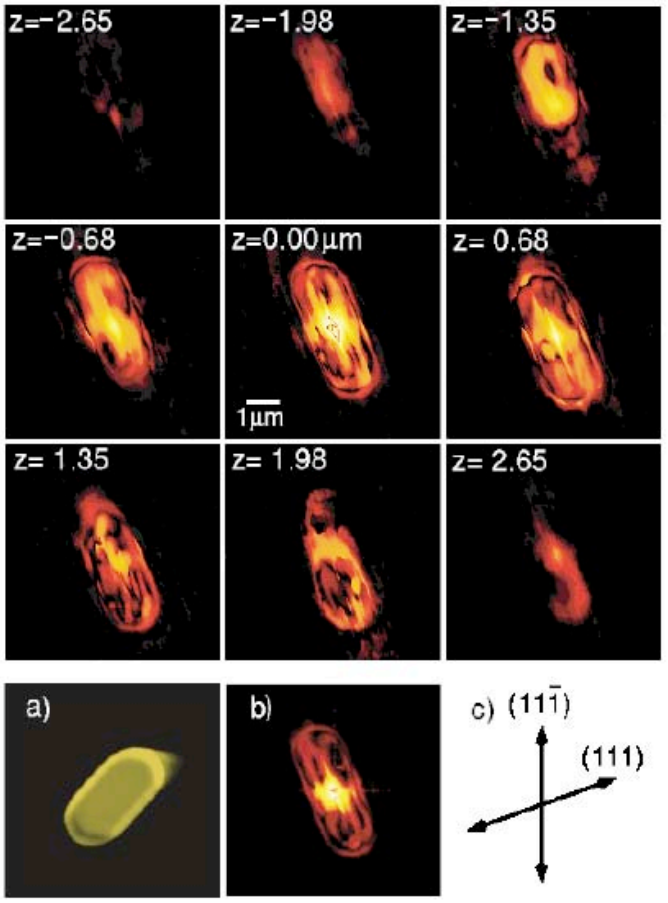

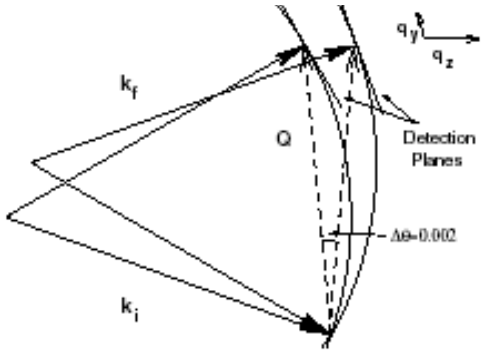

FIRST CDI RECONSTRUCTION USING A DEMONSTRATION OBJECT AT ESRF

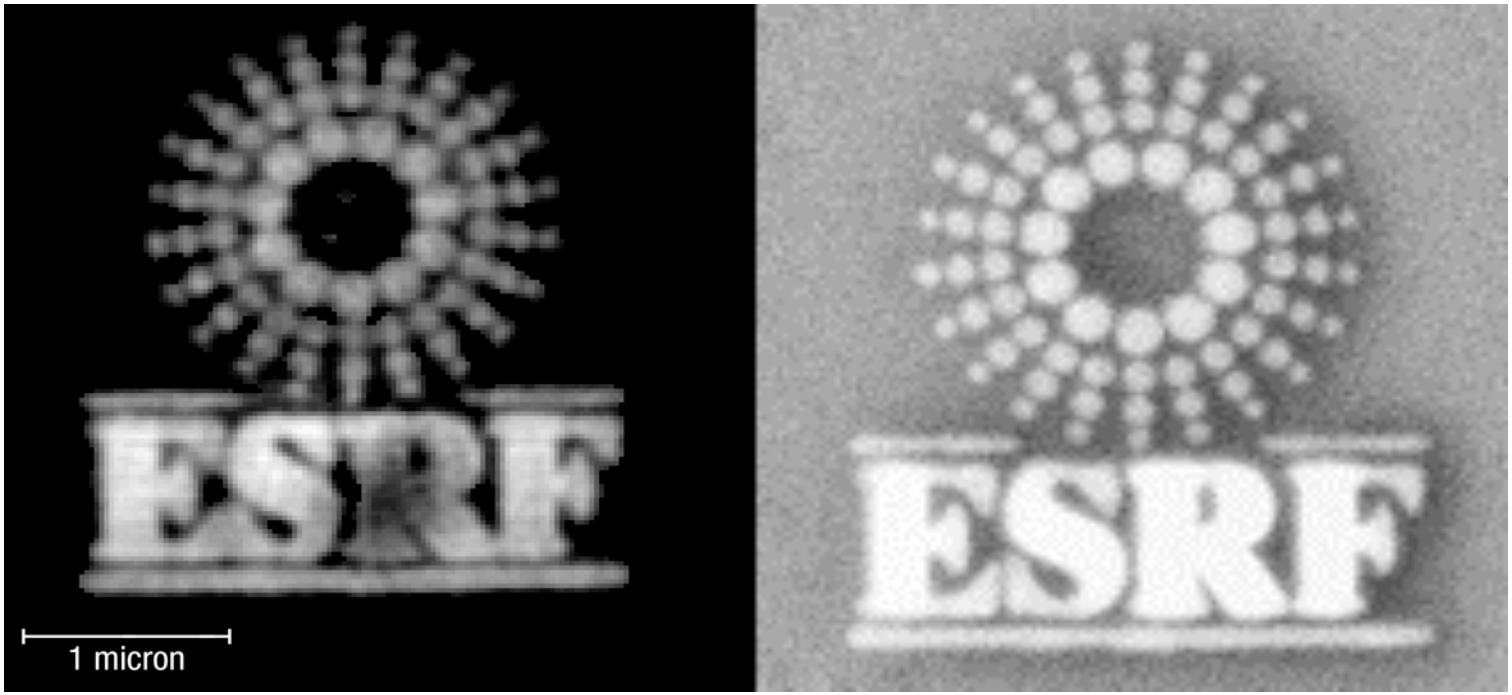

- Image recorded in air at ID10C at 8 keV
- Negative pattern using 40 nm tungsten foil
- Diffraction pattern extended to 22 nm resolution
- Left: reconstructed CDI image
- Right: SEM image

Slide courtesy of E. Lima

MOVIE SHOWING PROGRESSIVE CONVERGENCE OF THE ALGORITHM

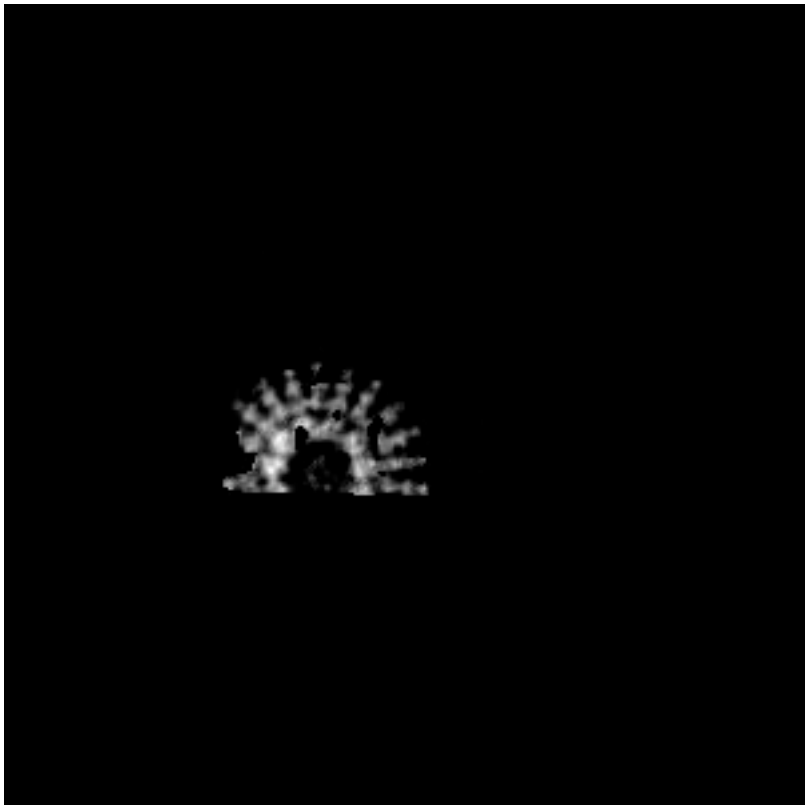

Slide courtesy of E. Lima

FIRST CXDI IMAGE OF A BIOLOGICAL SAMPLE

[Miao et al 2003]

- Imaging whole manganese-stained *escherichia coli* bacteria at λ = 2Å, resolution 30 nm

- Beginning of a pathway toward imaging low-contrast biological objects

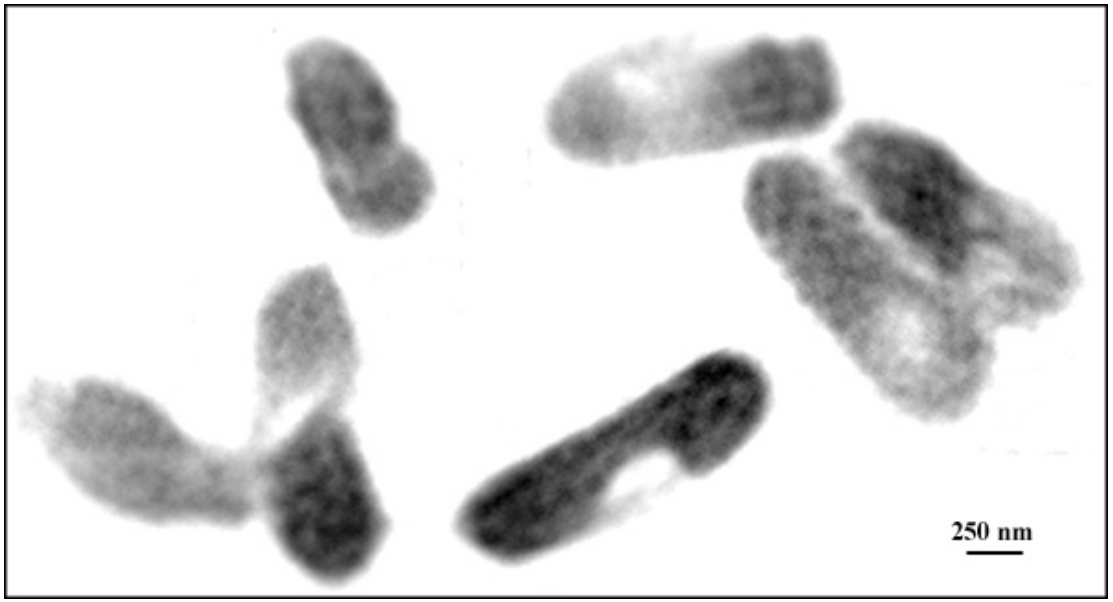

FREEZE-DRIED-YEAST-CELL RECONSTRUCTIONS

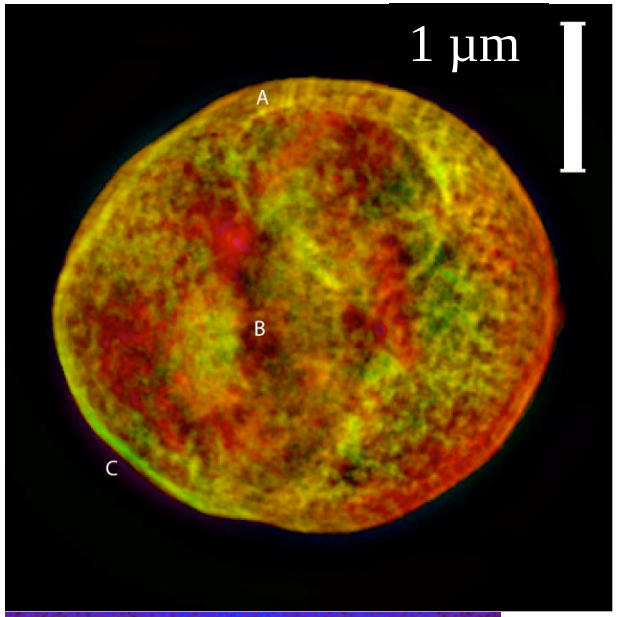

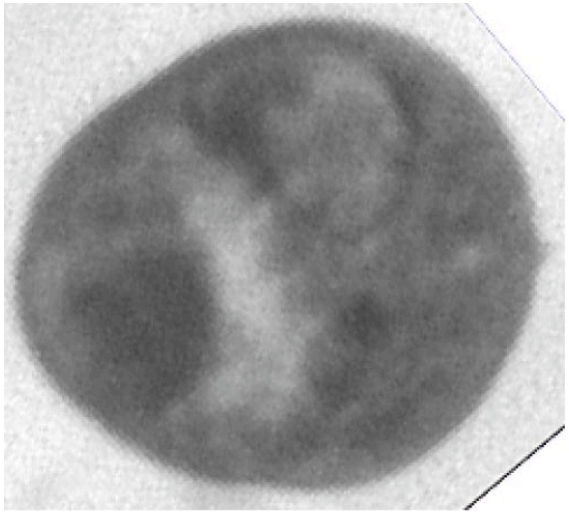

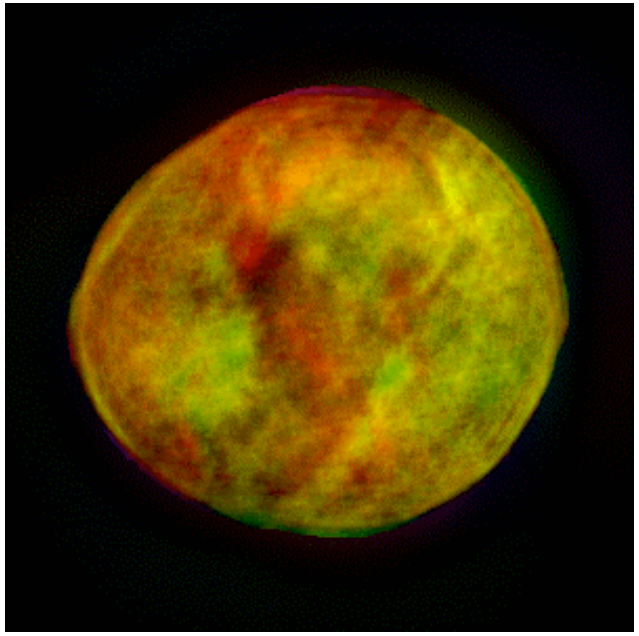

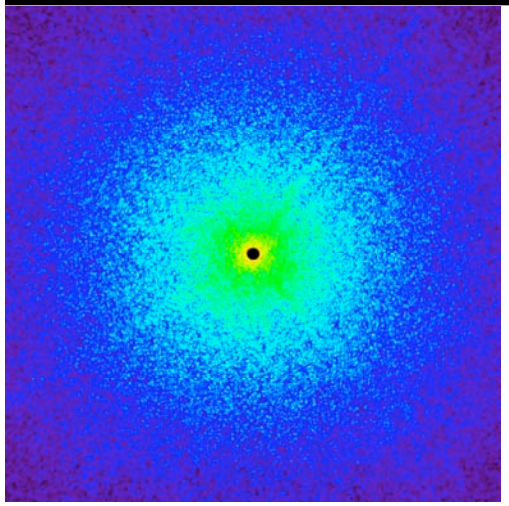

LEFT: Reconstruction of freeze dried dwarf yeast at a single tilt orientation. A: nucleus B: vacuole C: cell wall.

CENTER: STXM image of the same cell

RIGHT: movie of the nine reconstructions made

LOWER LEFT: Yeast cell diffraction pattern – 45 second total exposure – speckles are visble out to the corners which correspond to 13.4 nm spatial period (David Shapiro thesis project, work of SUNY/BNL and Cornell groups (PI's Kirz, Jacobsen, Cao, Elser))

FROZEN-HYDRATED YEAST SPORES RECONSTRUCTION

- E. Lima, PhD Thesis, Stony Brook University
- Unstained frozen-hydrated yeast spore, at 520 eV
- First CDI reconstruction of a frozen hydrated biological object

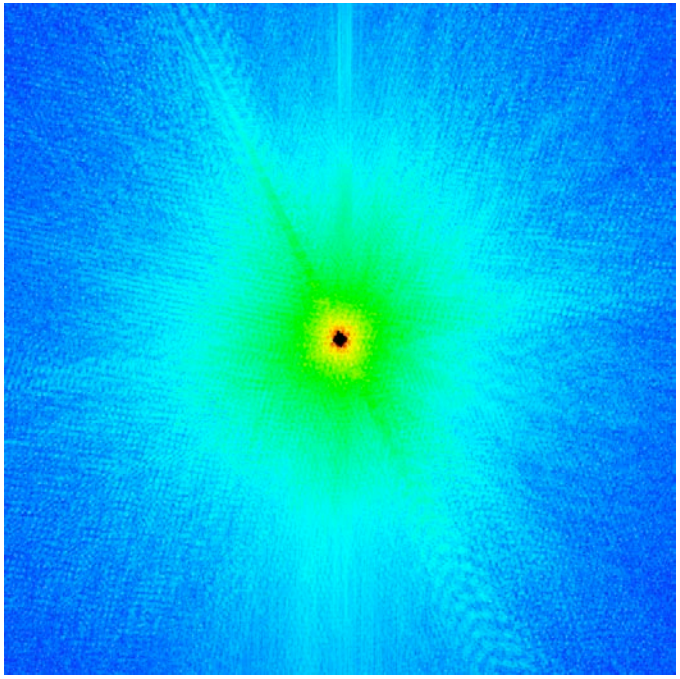

Signal extends to 25 nm
half-period

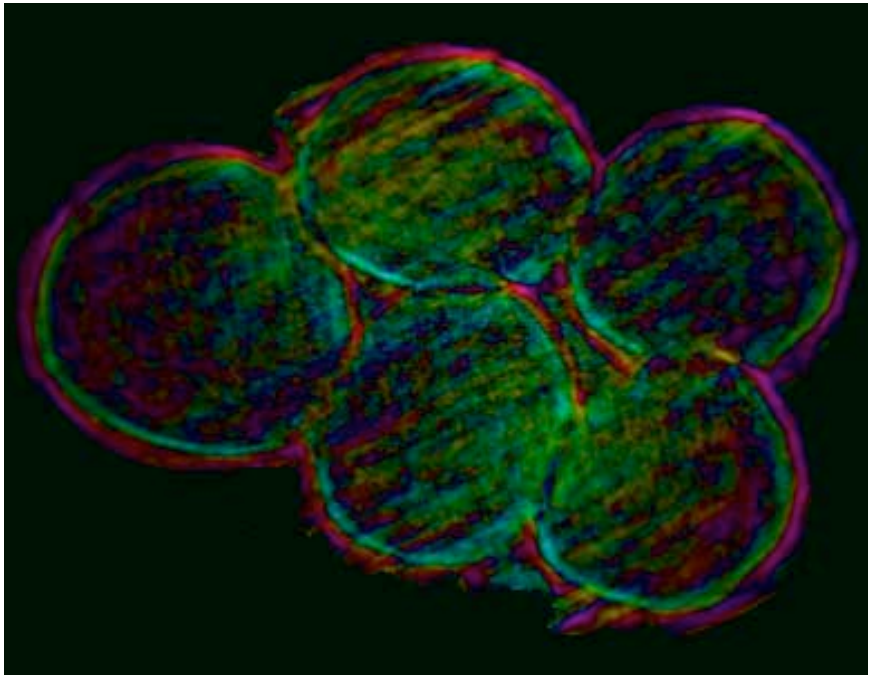

Brightness - amplitude
Hue - phase

FAR-FIELD DIFFRACTION

Object $f(x)$ which is non-zero only between the bounds of spacing W (known as the "support")

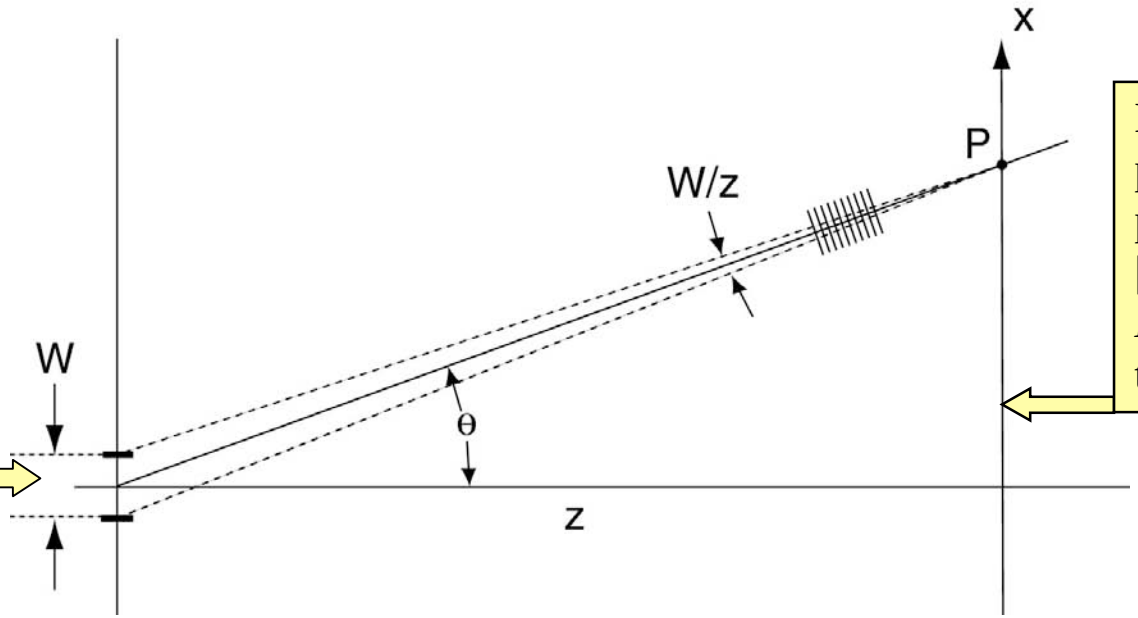

Diffraction pattern proportional to $|F(k)|^2$ where $F(k)$ is the transform of f

- In the far-field the x axis is a mapping of spatial frequency according to $k_P = \sin\theta/\lambda \cong x_P/(\lambda z)$
- The rays from the top and bottom of the object interfering at P produce Young's *intensity* fringes with a frequency $W/(\lambda z)$ - This is the highest frequency that can be present in the diffraction pattern
- According to the Shannon Sampling theorem the pattern (i. e. $|F(k)|^2$) must be sampled at twice that frequency in order to allow exact recovery of the pattern from the samples
- In other words a sampling interval of $\frac{1}{2}\frac{\lambda z}{W}$ is needed to avoid loss of information

MORE ABOUT SAMPLING

- In general the Shannon sampling theorem (aka the Kotelnikov theorem) states that, if a function $f(x)$ with transform $F(k)$ is bounded on one side with width W, then the function on the other side can be fully recovered from samples spaced at $1/W$
- Thus if f is bounded by W then the sampling interval for $F(k)$ should be

$$\Delta k \equiv \frac{\Delta x}{\lambda z} = \frac{1}{W} \quad \text{or} \quad \boxed{[\Delta x]_F = \frac{\lambda z}{W}}$$

- This is to be compared with the result from the last slide

$$\boxed{[\Delta x]_{|F|^2} = \frac{1}{2}\frac{\lambda z}{W}}$$

- Thus the Shannon sampling interval for the wave amplitude is twice that for the wave intensity

Therefore if the intensity pattern ($|F|^2$) is correctly (Shannon) sampled (i. e. not oversampled), and those data are used to get $|F|$, then $|F|$ will automatically be oversampled by a factor two in each dimension

Acta Cryst. (1952). **5**, 843

Some implications of a theorem due to Shannon.

By D. Sayre, *Johnson Foundation for Medical Physics, University of Pennsylvania, Philadelphia* 4, *Pennsylvania, U. S. A.*

(*Received* 3 *July* 1952)

Shannon (1949), in the field of communication theory, has given the following theorem: If a function $d(x)$ is known to vanish outside the points $x = \pm a/2$, then its Fourier transform $F(X)$ is completely specified by the values which it assumes at the points $X = 0, \pm 1/a, \pm 2/a, \ldots$. In fact, the continuous $F(X)$ may be filled in merely by laying down the function $\sin \pi aX/\pi aX$ at each of the above points, with weight equal to the value of $F(X)$ at that point, and adding.

Now the electron-density function $d(x)$ describing a single unit cell of a crystal vanishes outside the points $x = \pm a/2$, where a is the length of the cell. The reciprocal-lattice points are at $X = 0, \pm 1/a, \pm 2/a, \ldots$, and hence the experimentally observable values of $F(X)$ would suffice, by the theorem, to determine $F(X)$ everywhere, if the phases were known. (In principle, the necessary points extend indefinitely in reciprocal space, but by using, say, Gaussian atoms both $d(x)$ and $F(X)$ can be effectively confined to the unit cell and the observable region, respectively.)

For centrosymmetrical structures, to be able to fill in the $|F|^2$ function would suffice to yield the structure, for sign changes could occur only at the points where $|F|^2$ vanishes. The structure corresponding to the $|F|^2$ function is the Patterson of a single unit cell. This has twice the width of the unit cell, and hence to fill in the $|F|^2$ function would require knowledge of $|F|^2$ at the half-integral, as well as the integral h's. This is equivalent to a statement made by Gay (1951).

I think the conclusions which may be stated at this point are:

1. Direct structure determination, for centrosymmetric structures, could be accomplished as well by finding the sizes of the $|F|^2$ at half-integral h as by the usual procedure of finding the signs of the F's at integral h.

2. In work like that of Boyes-Watson, Davidson & Perutz (1947) on haemoglobin, where $|F|^2$ was observed at non-integral h, it would suffice to have only the values at half-integral h.

The extension to three dimensions is obvious.

References

Boyes-Watson, J., Davidson, E. & Perutz, M. F. (1947). *Proc. Roy. Soc.* A, **191**, 83.

Gay, R. (1951). Paper presented at the Second International Congress of Crystallography, Stockholm.

Shannon, C. E. (1949). *Proc. Inst. Radio Engrs., N.Y.* **37**, 10.

CONSEQUENCES OF SHANNON SAMPLING THE INTENSITY

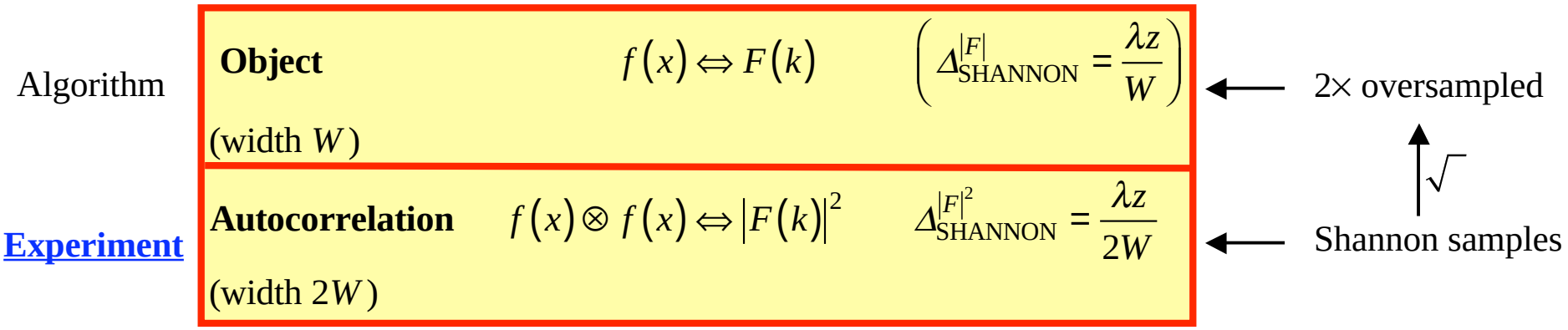

- Therefore $|F|$ derived from intensity data is twofold oversampled compared to its Shannon frequency (in each dimension)
- This means that f derived by transforming F will be zero padded to a width $2W$
- The zero-padded region allows "the support constraint" to be used
- This means that the algorithm is told that the electron density of the sample outside some given boundary is zero
- It seeks a solution for the phases of F in which (a) the support constraint is true in object space and (b) the measured values of $|F|$ are true in diffraction space

PHASE-RETRIEVAL ALGORITHMS: GENERAL SCHEME

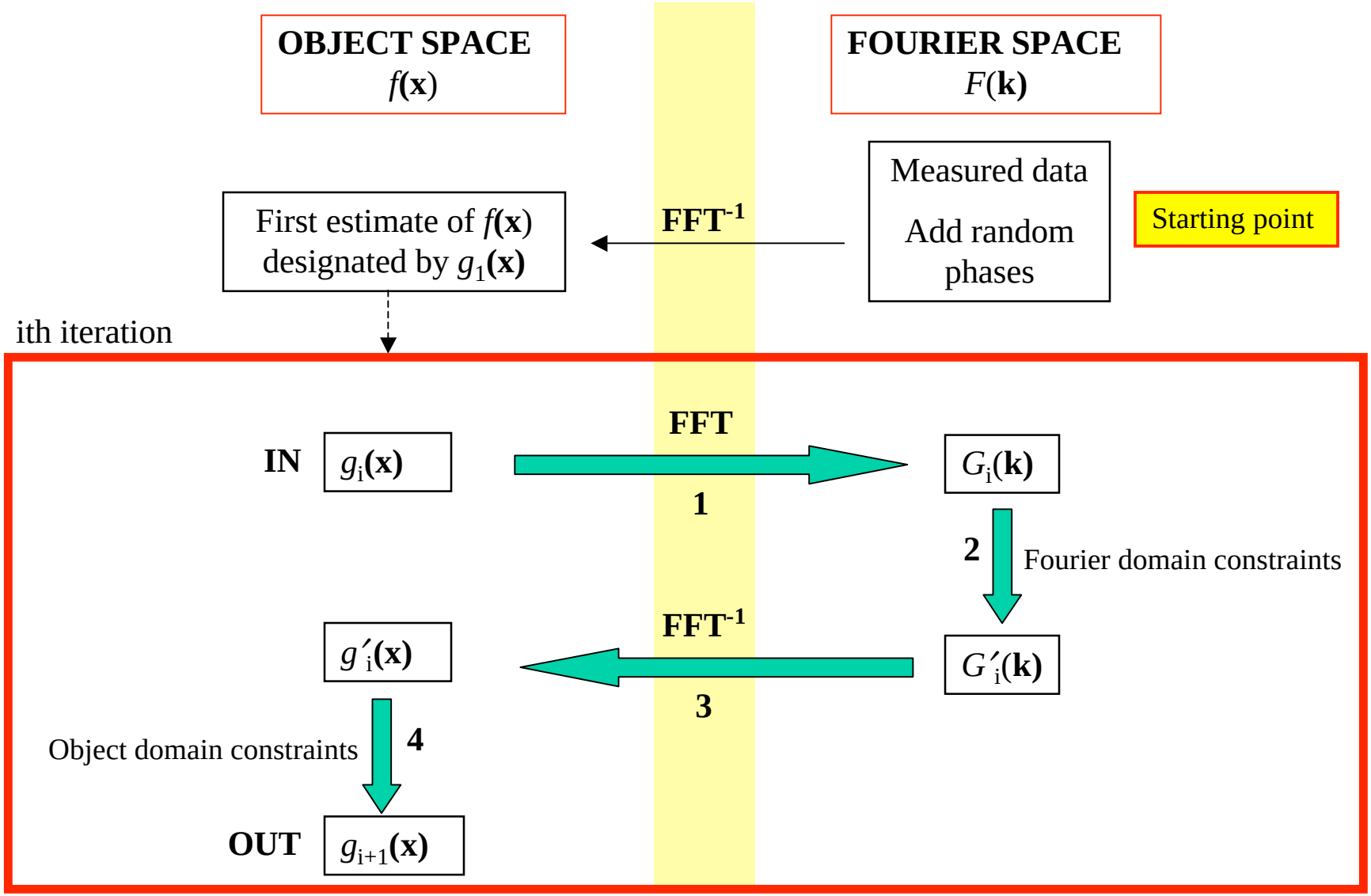

FIENUP HYBRID-INPUT-OUTPUT ALGORITHM STEPS

Dainty and Fienup 1985, S. Marchesini, *A unified evaluation of iterative projection algorithms for phase retrieval* Rev. Sci. Instrum. **78**, 011301 (2007)

Step 1 : $G_i(\mathbf{k}) = |G_i(\mathbf{k})| \exp[i\phi_i(\mathbf{k})] = \mathrm{FFT}[g_i(\mathbf{x})]$

Step 2 : $G'_i(\mathbf{k}) = |F(\mathbf{k})| \exp[i\phi_i(\mathbf{k})]$

INPUT

Step 3 : $g'_i(\mathbf{x}) = \mathrm{FFT}^{-1}[G'_i(\mathbf{k})]$

Step 4 : $$g_{i+1}(\mathbf{x}) = \begin{cases} g'_i(\mathbf{x}) & \mathbf{x} \notin S \\ g_i(\mathbf{x}) - \beta g'_i(\mathbf{x}) & \mathbf{x} \in S \end{cases}$$

OUTPUT

- S is the set of object domain points at which the object domain constraints are violated and β is a number normally between 0.5 and 1.0
- In the reconstructions from ALS and ESRF shown here, only this algorithm has been used
- The constraints we have used in the work reported here
  1. Object domain: support constraint (object must be zero outside an ***adaptive*** boundary)
  2. Fourier domain: Fourier amplitude equals the square root of the measured intensity
- We used no other constraints or prior knowledge - only the measured diffraction pattern

DESIGNING THE EXPERIMENT I: ARRANGING FOR SPATIALLY COHERENT ILLUMINATION OF THE SAMPLE

- One can show that the speckles will not be significantly blurred if the full-angle spread of the illuminating beam $\Delta\vartheta$ satisfies $\Delta\vartheta.2W = \lambda/2$ [Spence et al 2004] - W and λ are known
- This is a spatial coherence condition that says roughly that the sample plus the zero-padded area has to be coherently illuminated
- Choose a pinhole (or equivalent set of slits) of width about $2W$
- Choose a distance downstream of the pinhole at which the beam has widened (diffracted by $\Delta\vartheta$) to about three or four pinholes diameters and place the sample (place guard slits in between the pinhole and sample)
- The idea is that the beam will be wide enough that the sample will stay in the beam even when displaced by the run-out of the rotation stage but not so wide that a lot of flux is lost
- Note that it is not necessary that the beam is a single mode - only that whatever part is used to illuminate the sample plus zero-padded area should be single mode

DESIGNING THE EXPERIMENT II: TEMPORAL COHERENCE (MONOCHROMATICITY) REQUIREMENTS

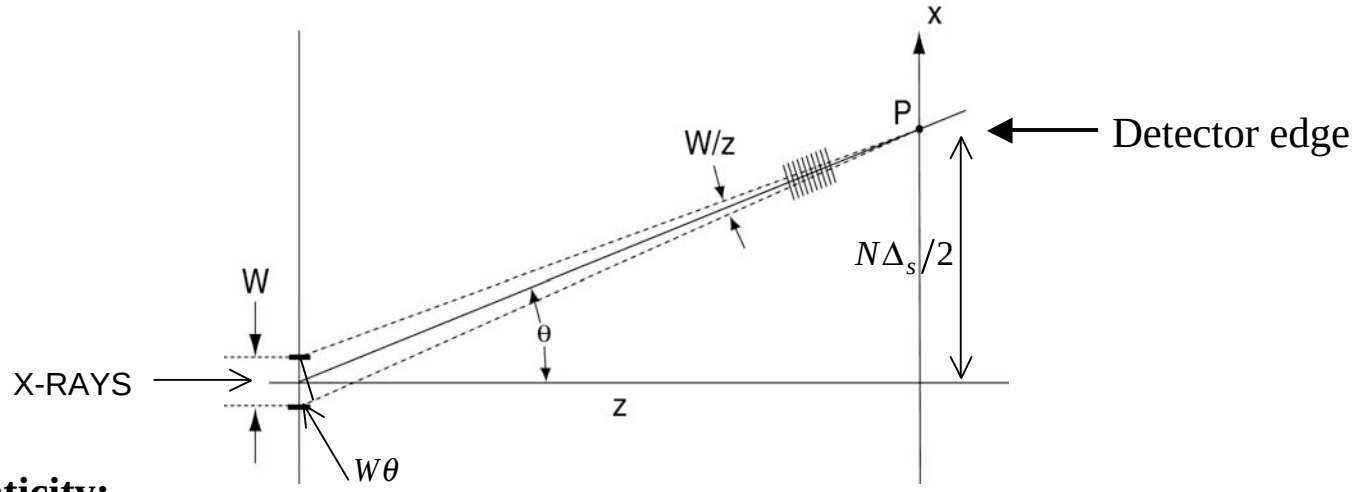

Monochromaticity:

1. Assume that the detector has *NxN* pixels each of width equal to the Shannon interval $\Delta_s = \lambda z/(2W)$
2. Also from the diagram $\theta = N\Delta_s/(2z)$
3. The greatest (worst case) path difference between two interfering signals at the detector edge is $W\theta$
4. To ensure at least 50% overlap of the interfering wave trains we must require the coherence length $\lambda^2/(\Delta\lambda) \geq 2W\theta$ so substituting we get

$$\frac{\lambda}{\Delta\lambda} \geq \frac{2W\theta}{\lambda} = \frac{2W}{\lambda}\frac{N\Delta_s}{2z} = \frac{2W}{\lambda}\frac{N}{2z}\frac{\lambda z}{2W} = \frac{N}{2}$$

or $\boxed{\frac{\lambda}{\Delta\lambda} \geq \frac{N}{2}}$

DESIGNING THE EXPERIMENT III: CHOICE OF WAVELENGTH

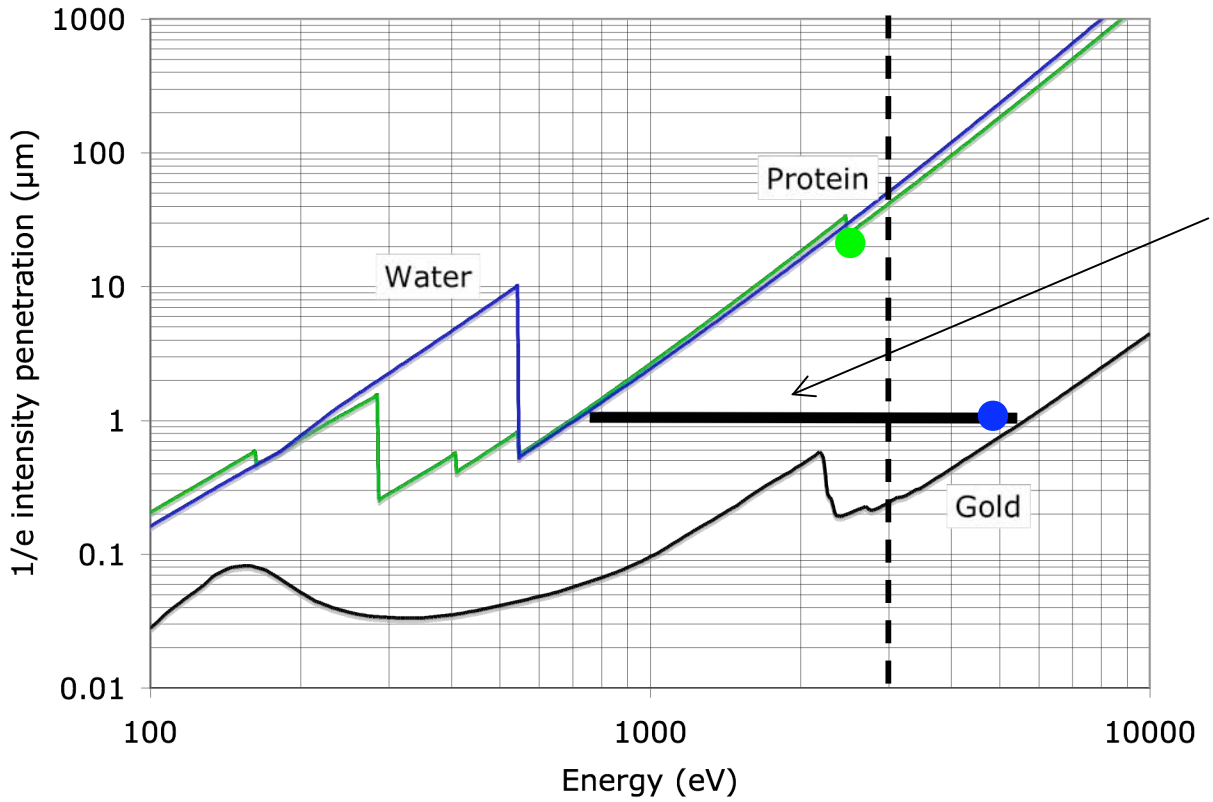

3 keV is sufficient for 10-20 μm objects of biological density but there is a size/density region that needs a higher energy

DESIGNING THE EXPERIMENT III: CHOICE OF WAVELENGTH (continued)

FLUX CONSIDERATIONS:

- The exposure time on a given source increases like E^4 - conclusion: use lowest possible energy

DOSE CONSIDERATIONS:

- The dose for light elements (biology say) is roughly flat with wavelength

DIFFRACTION CONSIDERATIONS:

- For a maximum diffraction angle of 15° (Bragg angle of 7.5°) - 2.5 keV (0.5 nm wavelength) is enough to get to 1 nm resolution

RECONSTRUCTION CONSIDERATIONS

- Harder x-rays will make the scattering factors essentially real which favors higher-energy x-rays

COMPUTER POWER

- 3D reconstruction is also limited by computer power - currently 10 hours for $(1k)^3$ - this should reduce the demand to measure big objects

ALS BEAM LINE 9.0.1: COHERENT OPTICS

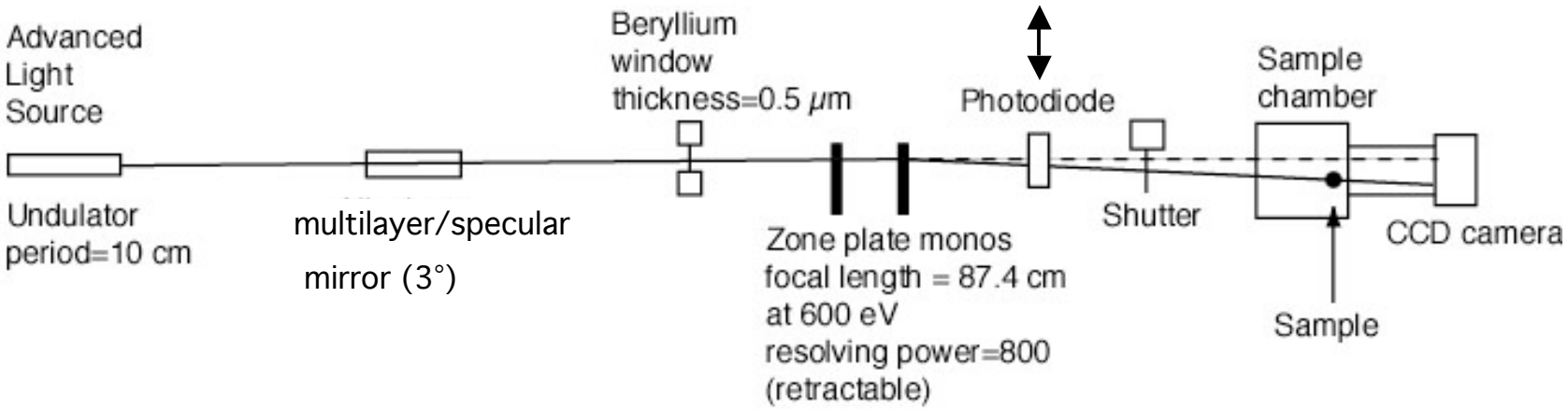

BEAM LINE SIDE VIEW (NOT TO SCALE)

RATIONALE:

- Experiments have been done at 520, 750 and 1500 eV in undulator 3rd harmonic
- Be window is 0.8 mm diameter which defines the beam size
- XPCS users originally required pink beam so zone plate mono is retractable
- Resolving power of 500-1000 is required (compared to ≈100 for the pink beam)

THE STONY BROOK DIFFRACTION CHAMBER ALLOWS ACCURATE SAMPLE ROTATION AND DATA ACQUISITION

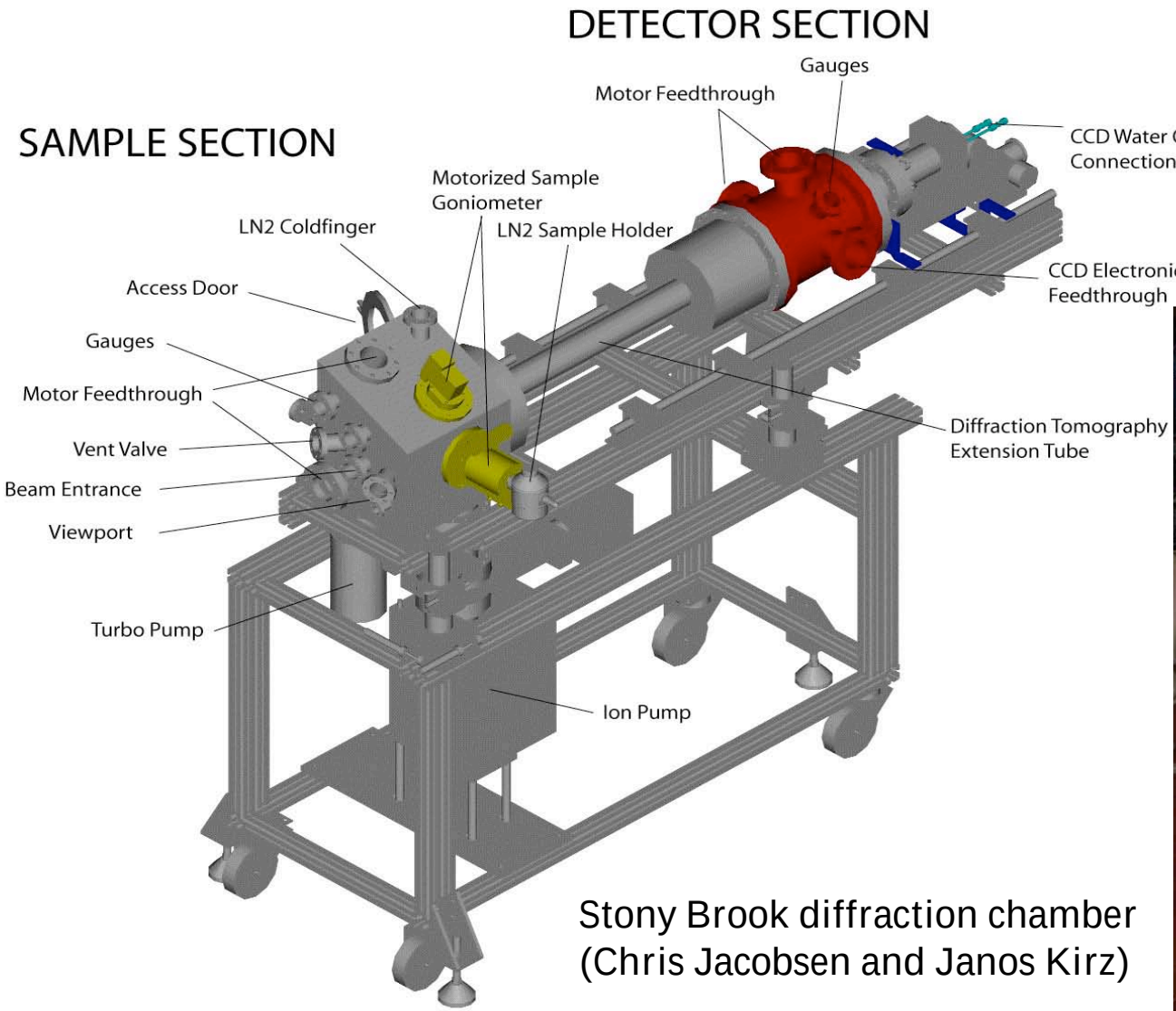

Stony Brook diffraction chamber
(Chris Jacobsen and Janos Kirz)

Installed at ALS BL9.0.1

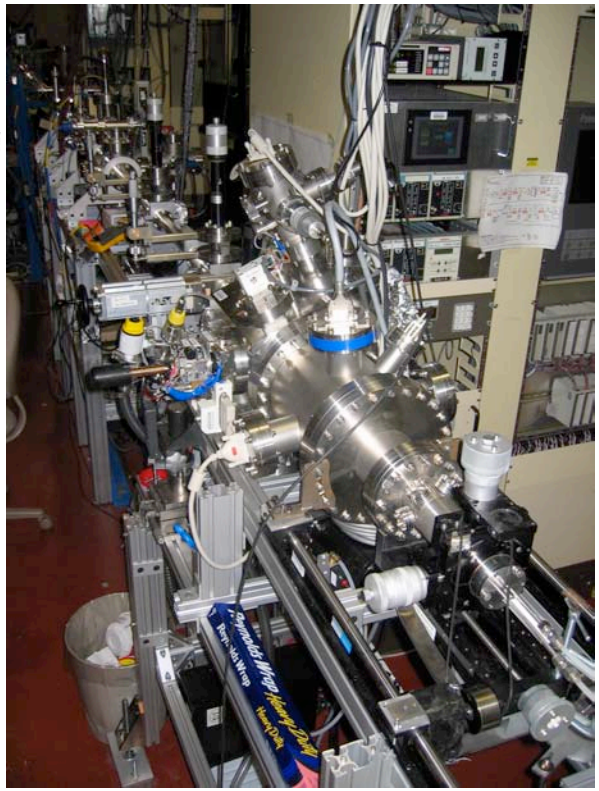

DIFFRACTION CHAMBER OPTICAL ELEMENTS

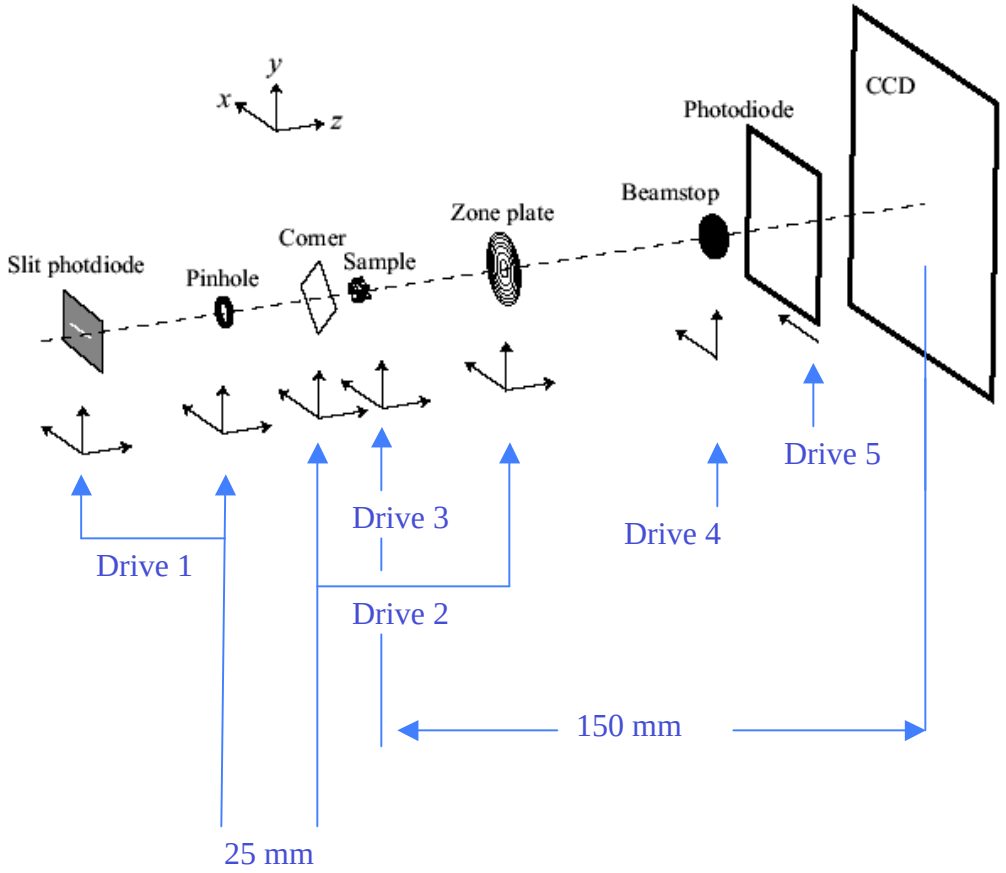

Slide courtesy D. Shapiro

NATURAL COCCOLITH SAMPLE - HOW DO WE KNOW WE ARE REALLY ILLUMINATING THE SAMPLE

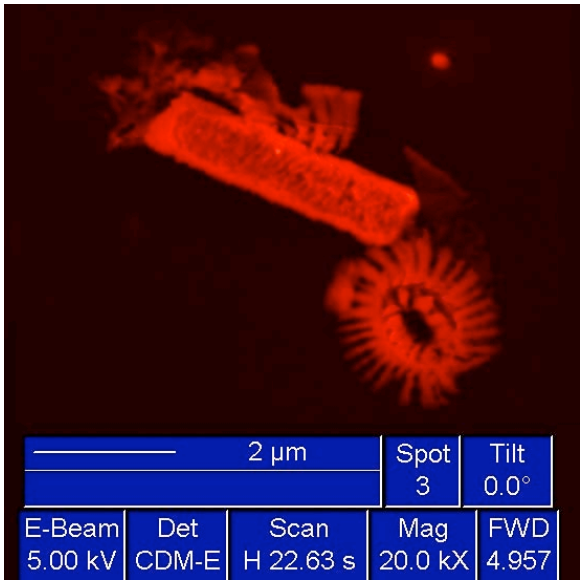

- Coccolith, calcite shields produced by unicellular marine algae (haptophytes) (SEM picture)
- The sample was placed on a Si_3N_4 membrane with focused ion beam (FIB).
- The dot on the up right corner is a deposited platinum tower about 100 nm diameter and 400 nm high
- The dot can be as a reference for Fourier transform holography

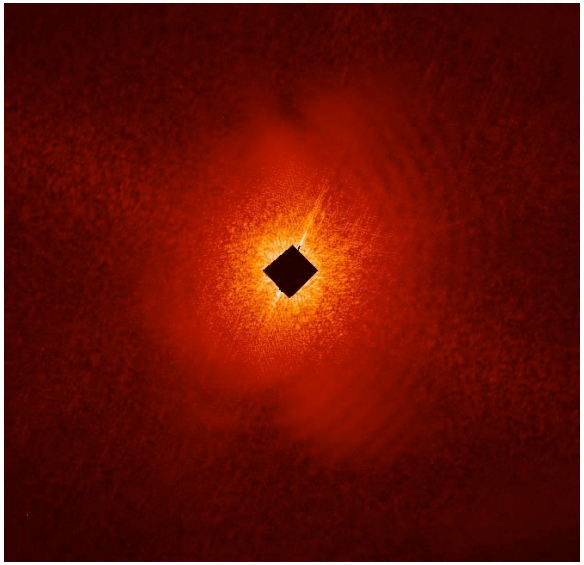

A diffraction pattern (Fourier transform hologram in this case) taken with an exposure time of 20 seconds

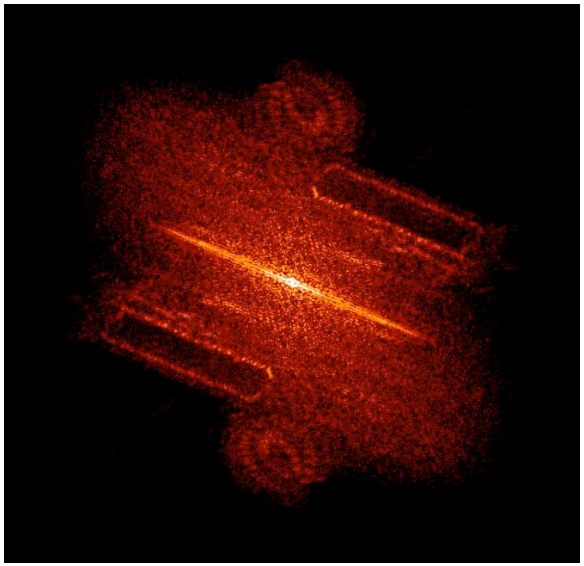

Autocorrelation function of the left pattern

GATAN 630 CRYO HOLDER

Slide: courtesy T. Beetz, Xradia

High-tilt cryo holder for JEOL TEM which allows use of special slotted sample grid that allows tilts to ±80° without obstructing the beam or spilling the LN2

JEOL TEM GONIOMETER: SCHEMATIC

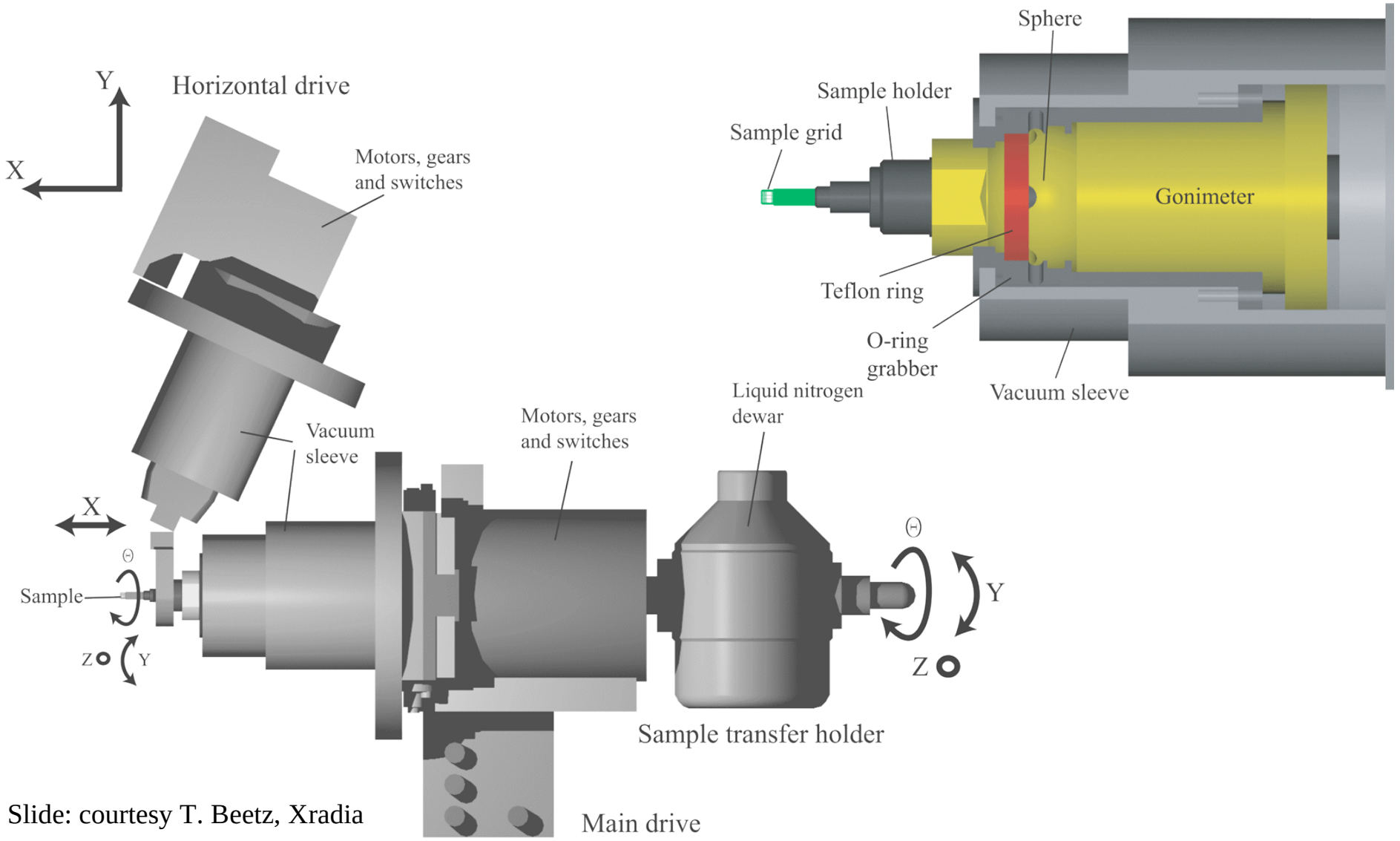

Slide: courtesy T. Beetz, Xradia

ELECTRON SAMPLE PREPARATION METHODS FOR BIOLOGICAL SAMPLES AS USED AT ALS

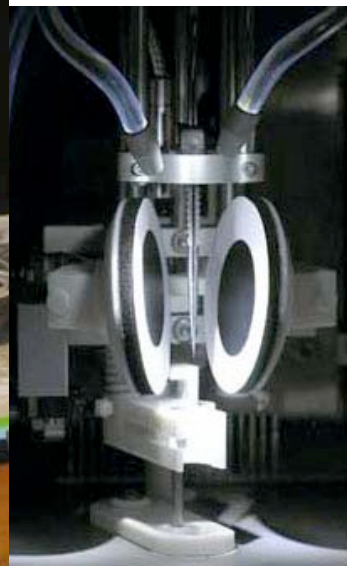

Grids with live cells are

- Taken from culture medium and blotted
- Plunged into liquid ethane (cooled by liquid nitrogen) to freeze the water in the sample to vitreous ice (at ESRF a home made plunger (Lima/Wiegart) is used)
- Loaded into cryo holder
- Concerns exist about how large a sample can be vitrified in this way
- People move from electron techniques to x-ray to look at bigger samples - but how big can they be and still plunge freeze successfully?
- It may be necessary to turn to pressure freezing which can work slowly and can still freeze big objects (>0.1 mm)

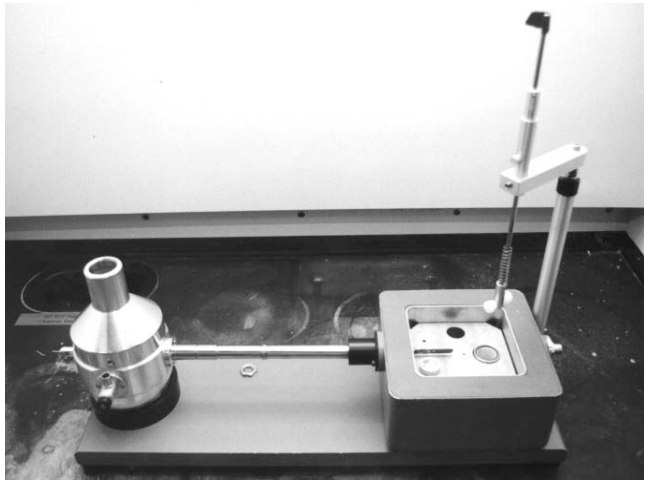

Slide: A. Stewart (Stony Brook)

FROZEN HYDRATED: STABLE SPECIMENS!

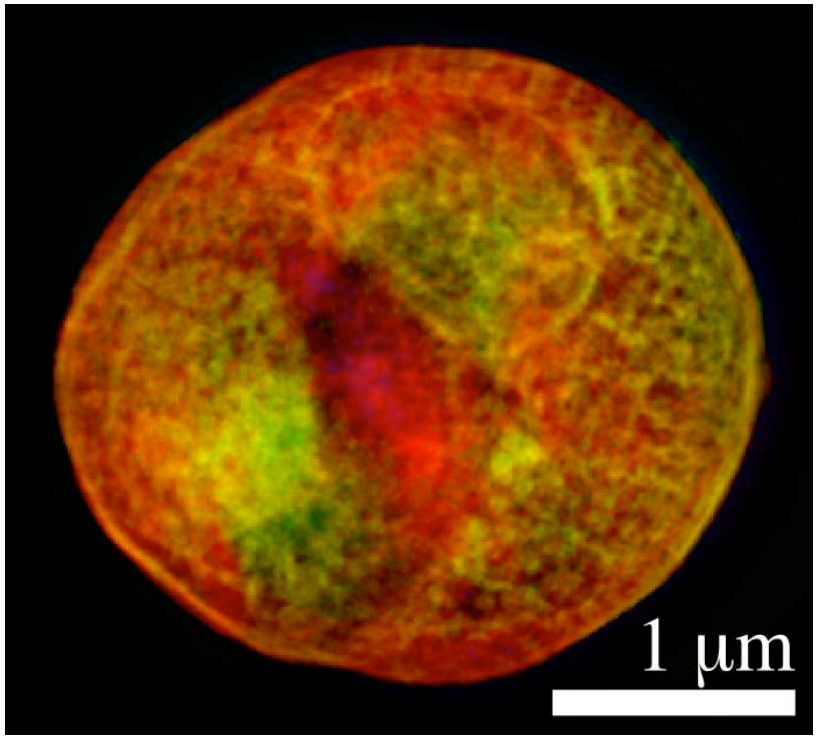

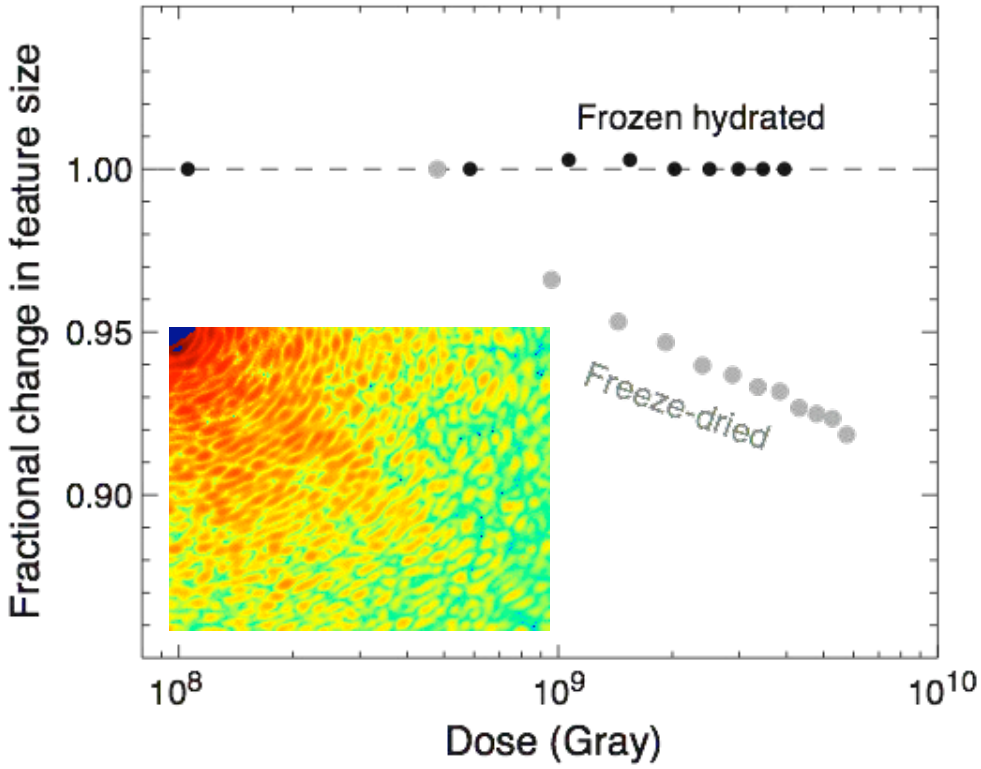

Reconstructed freeze dried yeast cell

(David Shapiro, PhD dissertation, Stony Brook, 2004)

Frozen hydrated specimens don't shrink in the beam (freeze-dried specimens do)

Slide: courtesy A. Stewart (Stony Brook)

DIFFRACTION PATTERN FROM FROM UNSTAINED FROZEN-HYDRATED BACTERIA (E. LIMA and L. WIEGART)

Deinococcus Radiodurans Bacteria:

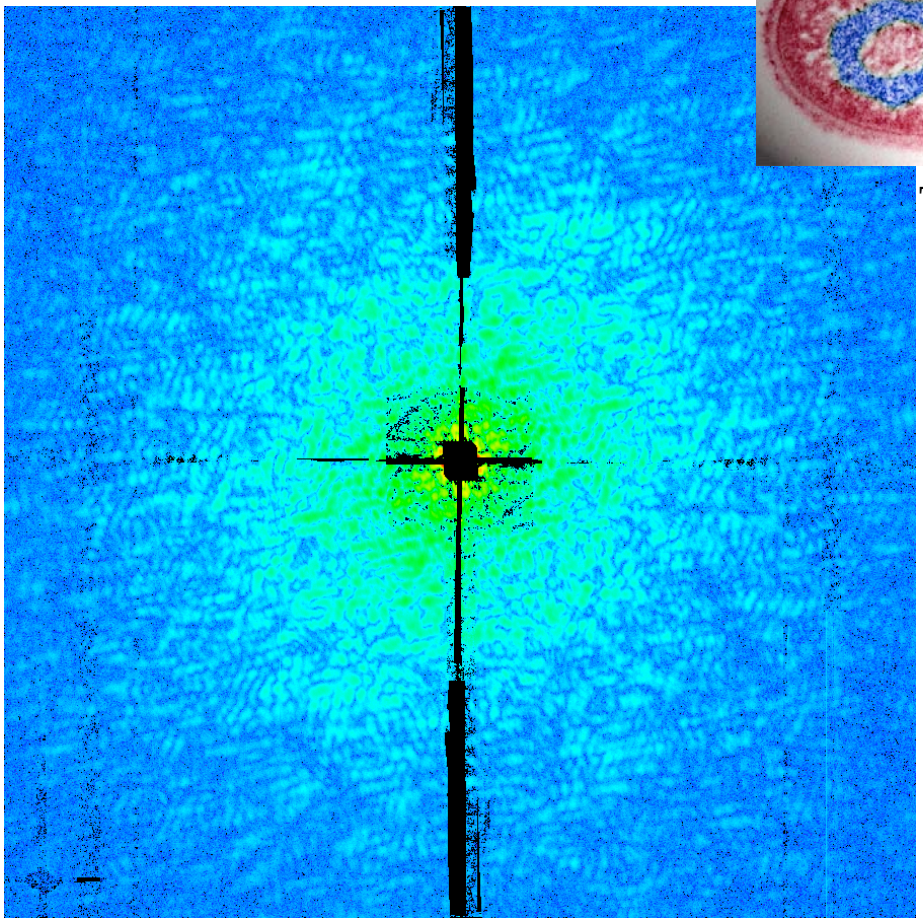

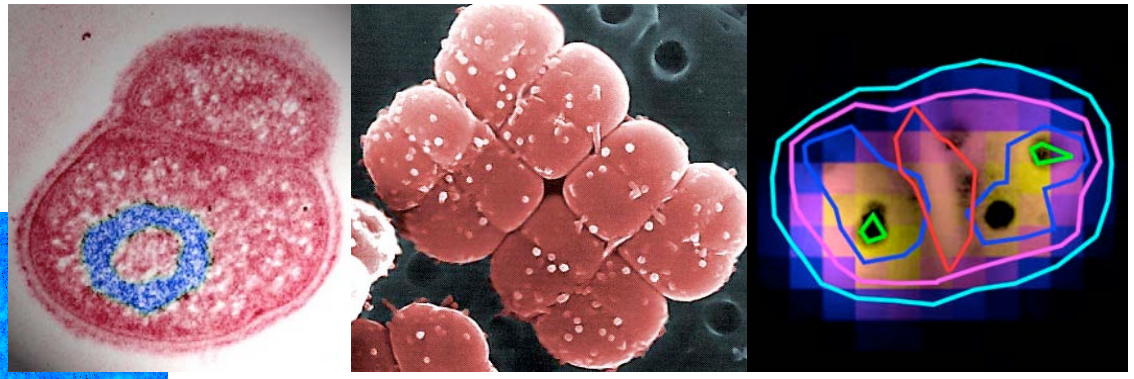

TEM SEM XRF

- X-ray energy = 8 keV
- Partial CCD chip 900x900
- signal to 12 nm (resolution) half-period
- 35 min total exposure
- using crl focusing
- $3x10^8$ photons/sec/10x10 µm field
- Very good quality data but not yet reconstructed

Slide courtesy E. Lima ESRF

DATA ACQUISITION IN AIR USING 8KEV X-RAYS (E. LIMA and L. WIEGART

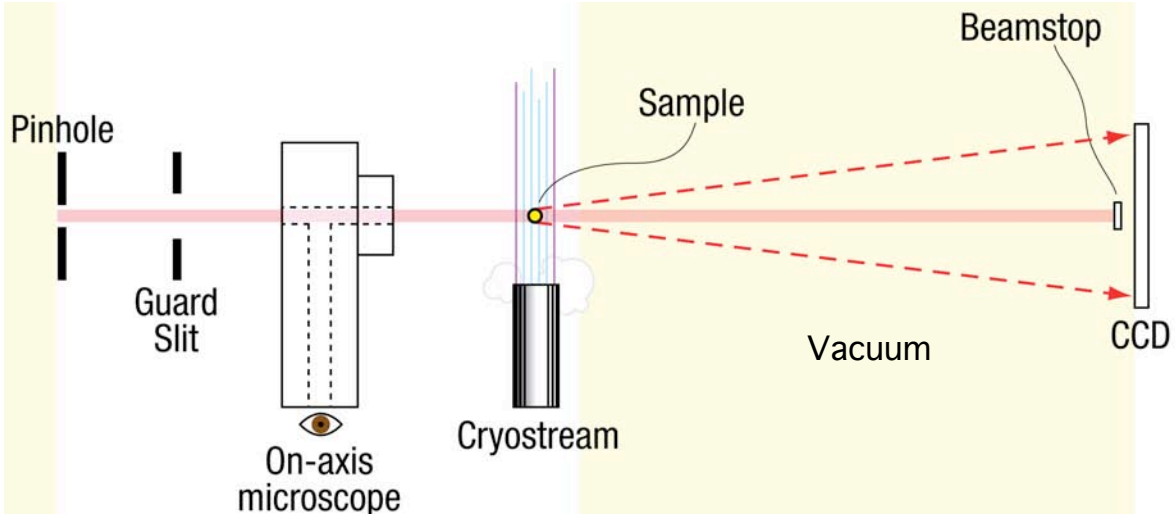

- Data taken at ID10C mostly at 8 keV
- Frozen samples are protected from ice contamination within cryostream
- Samples are monitored between data-taking runs by on-axis light microscope

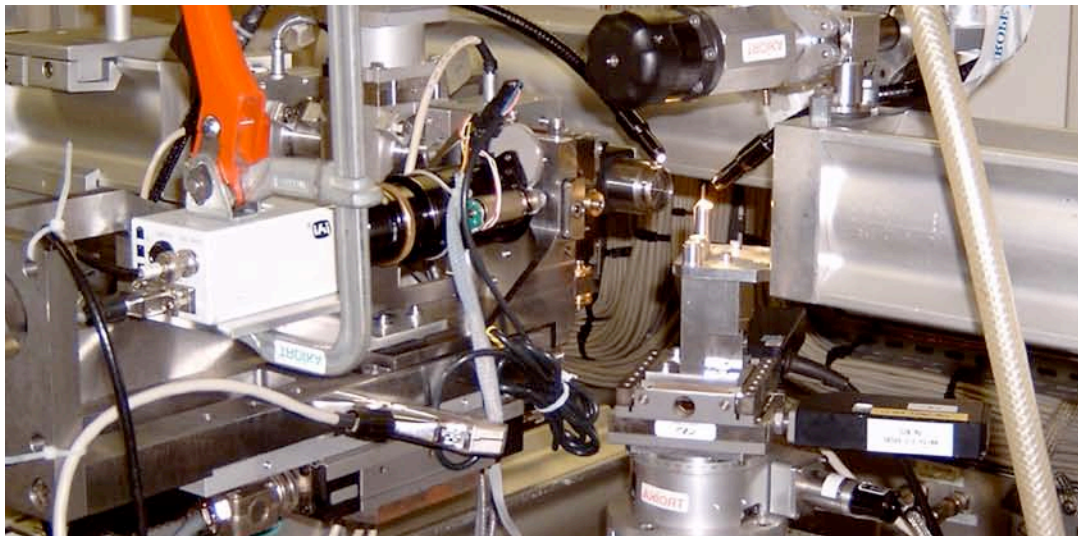

Slide courtesy E. Lima ESRF

SAMPLE PREPARATION AND MOUNTING
(E. LIMA and P. PERNOT)

Powder diffraction data demonstrates vitreous ice after plunge-freezing

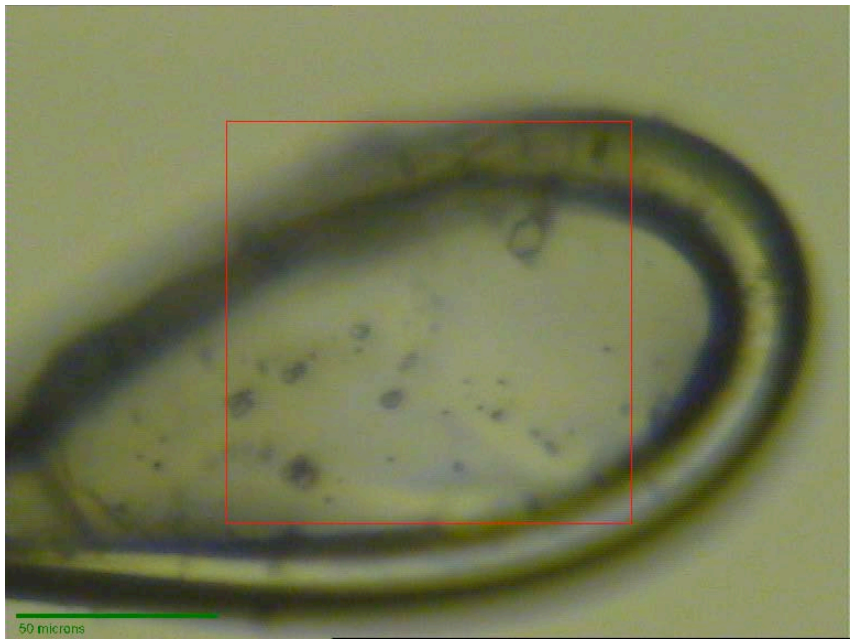

Nylon sample loop
Red square=ID14 beam size
(100x100 μm^2)

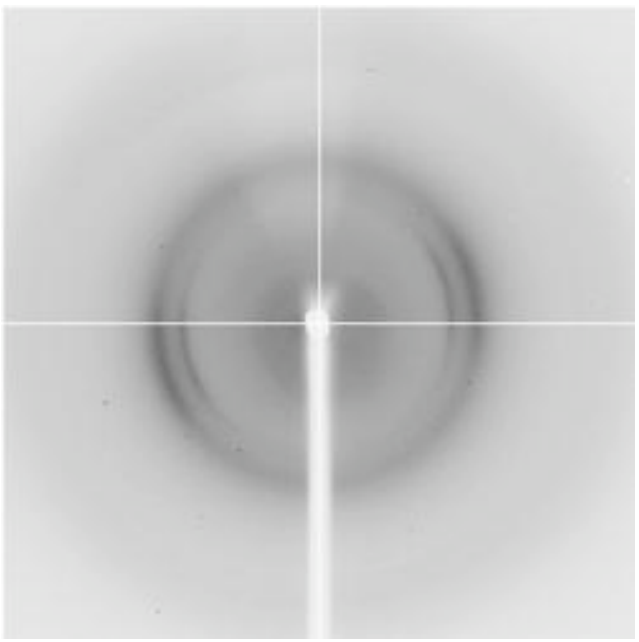

Powder diffraction at 13 keV
ID14, ESRF

Slide courtesy E. Lima ESRF

DEMONSTRATION OF HIGH-RESOLUTION CXDI ON A GOLD-BALL SAMPLE

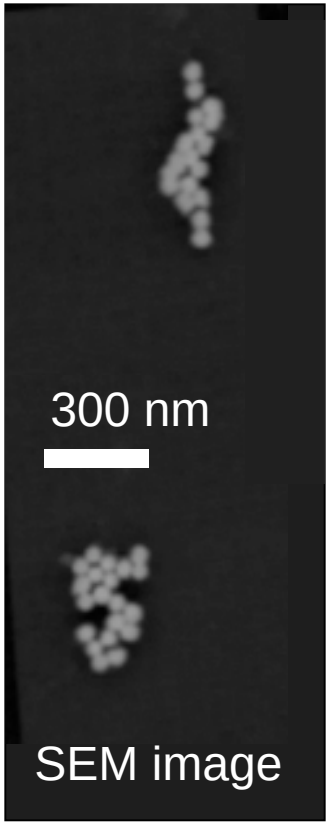

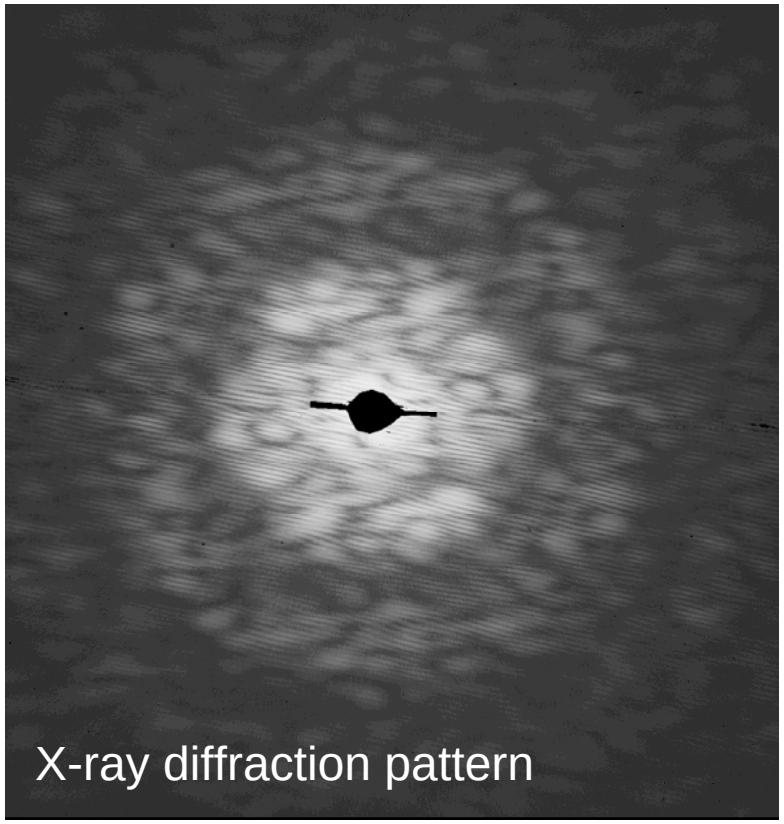

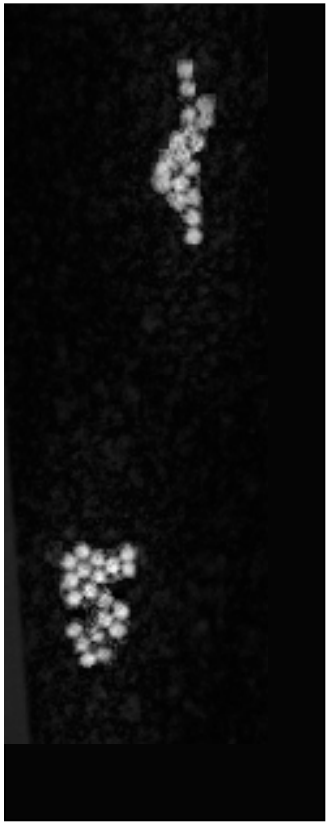

- Sample: 50 nm gold spheres
- Diffraction recorded with undulator radiation, $\lambda = 1.6$ nm
- Rayleigh resolution of reconstructed image: 10 nm
- Reconstruction performed with Shrinkwrap: a variation of Fienup-hybrid-input-output algorithm, with dynamic support constraint [S. Marchesini et al PRB 2003]

LENSLESS IMAGING WITH THE "SHRINKWRAP" ALGORITHM

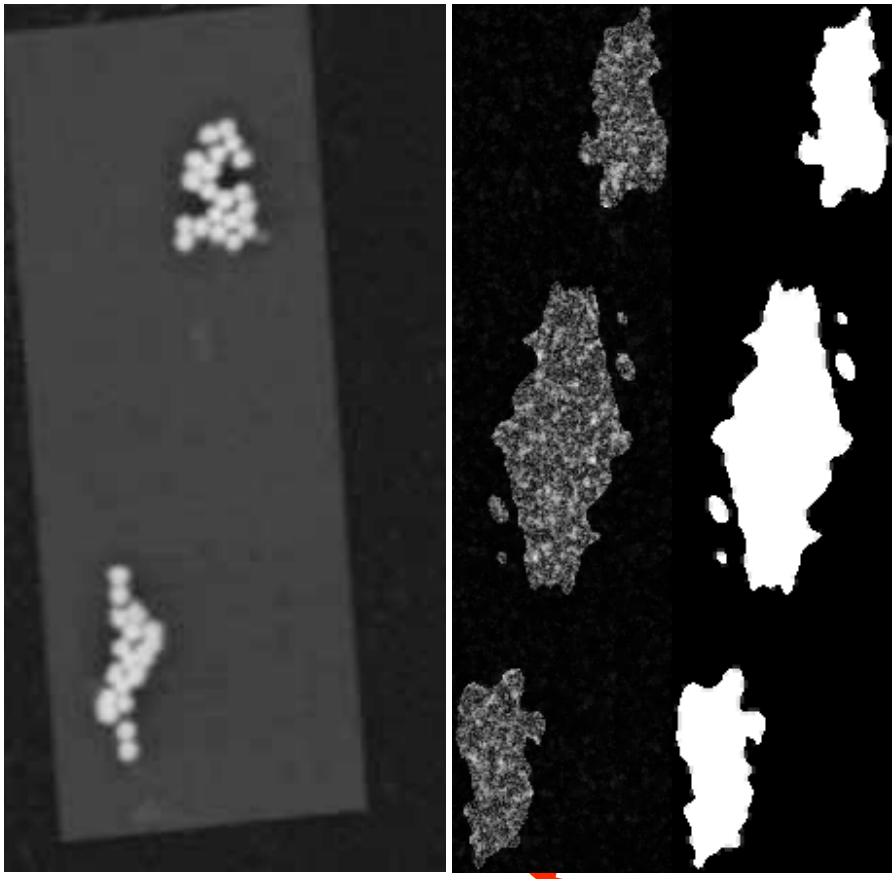

Scanning electron microscope image

First estimate of the support function

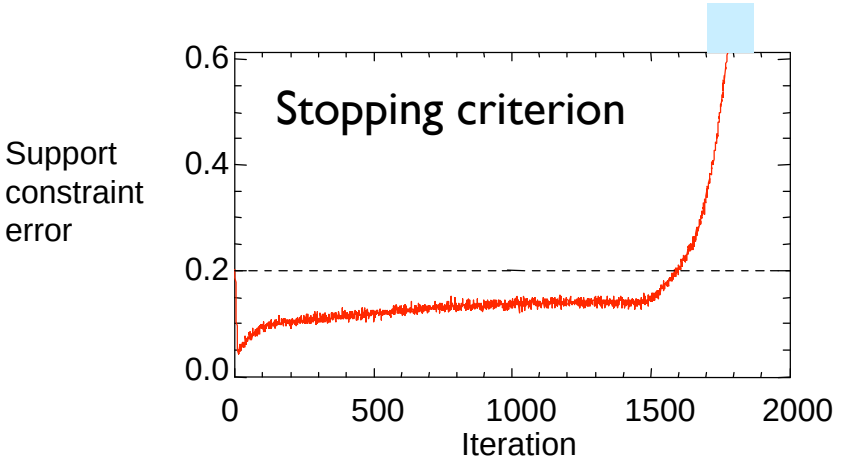

Marchesini *et al.,* Phys. Rev. B 68 140101, (2003)

First estimate of the object: thresholded autocorrelation function (transform of the measured data)

WE MANUFACTURED A COMPACT 3D TEST OBJECT

Lawrence Livermore Lab group:

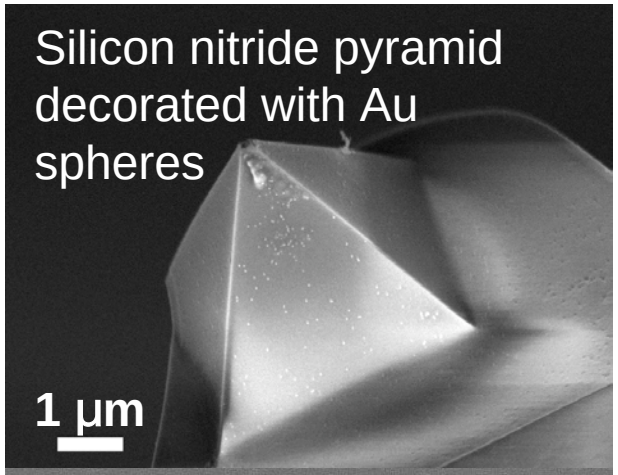

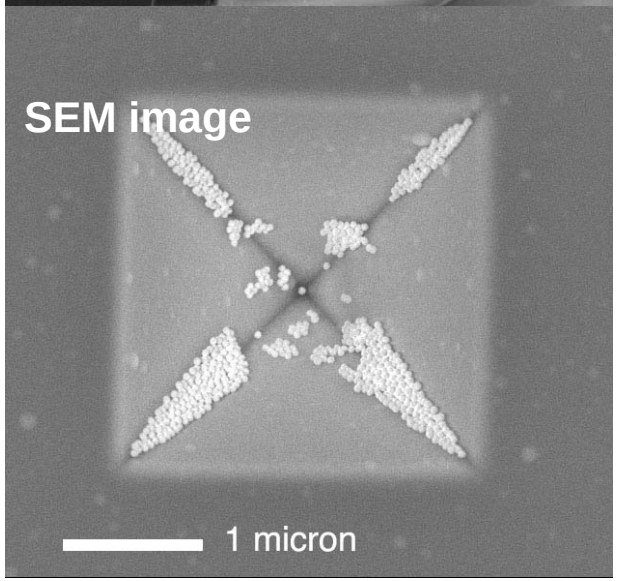

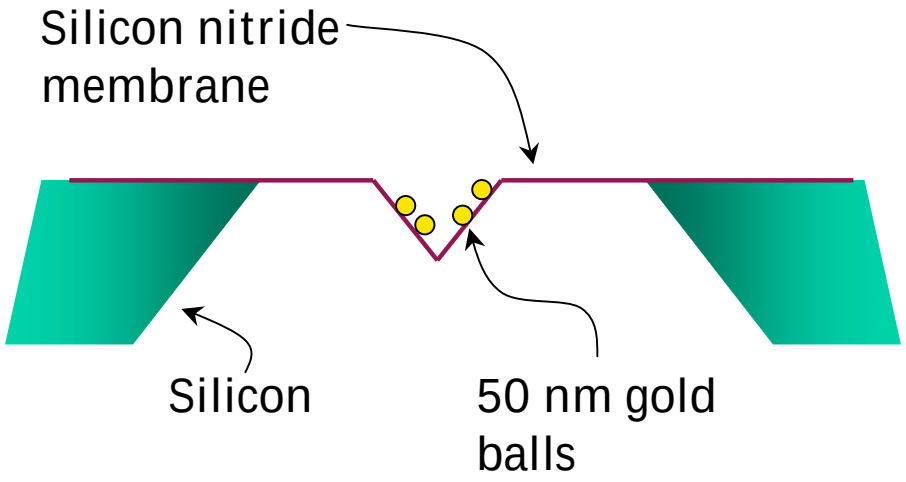

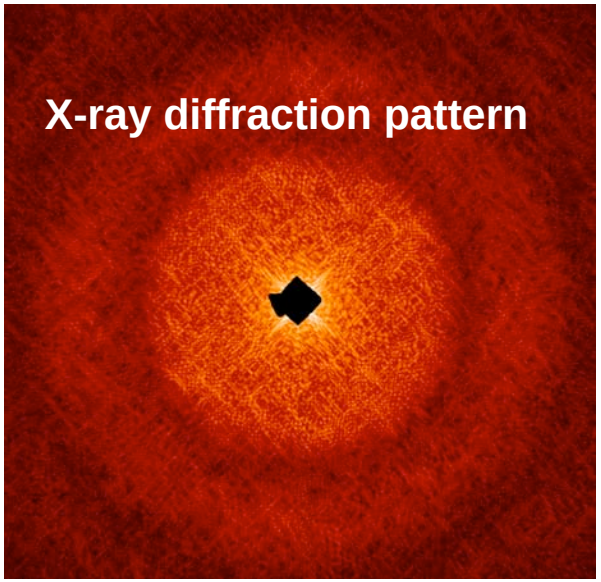

FULL 3D X-RAY RECONSTRUCTION OF NON-CRYSTALLINE MATERIAL AT HIGH RESOLUTION - ANTON BARTY, LLNL

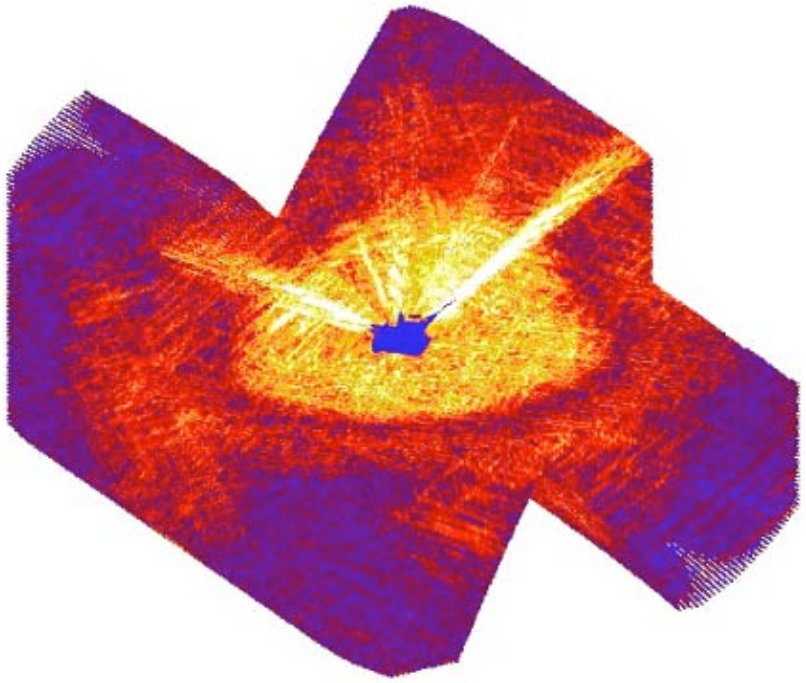

Coherent X-ray diffraction data, rotating the sample -57 to +65 degrees (5×10^8 data points)

Complete image reconstruction achieved, without any prior knowledge, using **Shrinkwrap**, **parallelized** for 3D on 16-node cluster.

Slide courtesy A. Barty LLNL

WITH A FULL 3D RECONSTRUCTION IN HAND WE CAN GET REAL-SPACE PROJECTIONS USING A SLICE THROUGH *k*-SPACE

Anton Barty, LLNL

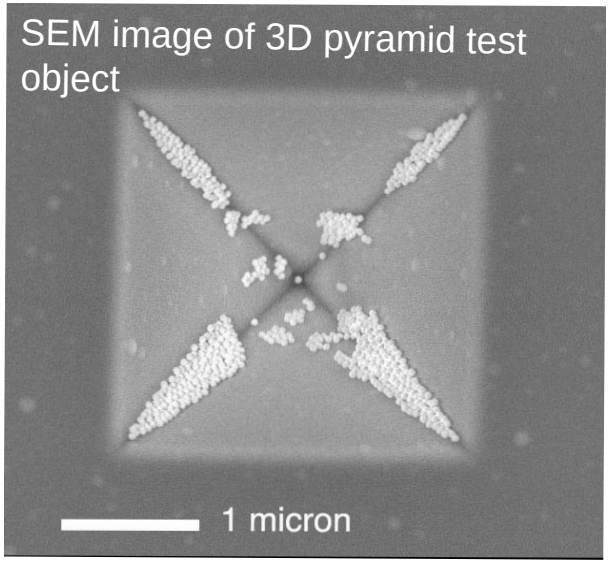

Projected views from the 3D reconstruction

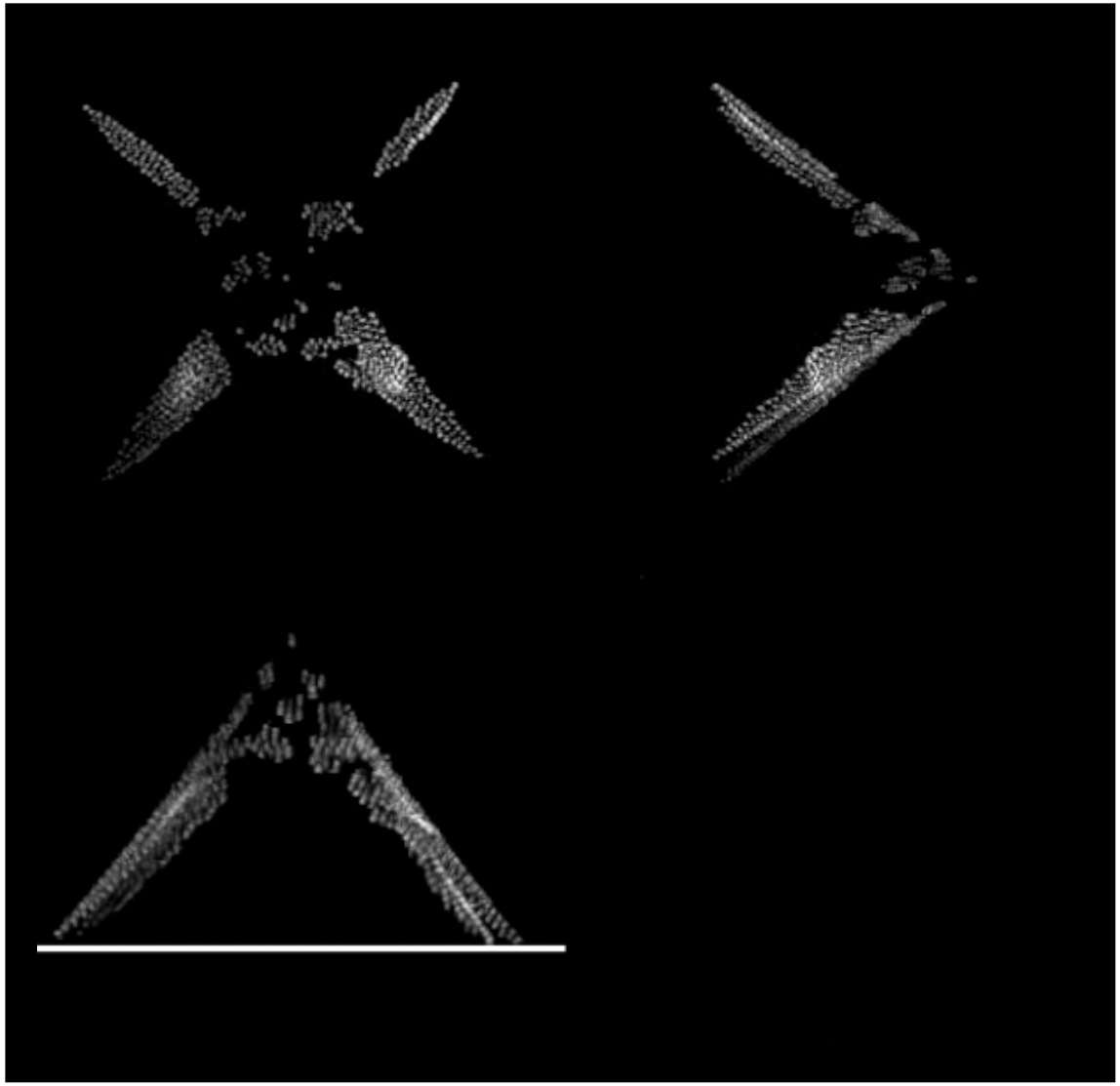

Slide courtesy A. Barty LLNL

MEASURES OF RESOLUTION: REAL SPACE

H. Chapman et al, J. Opt. Soc. Am. A **23,** 1179-1200 (2006)

3 orthogonal line-outs of a single 50 nm ball

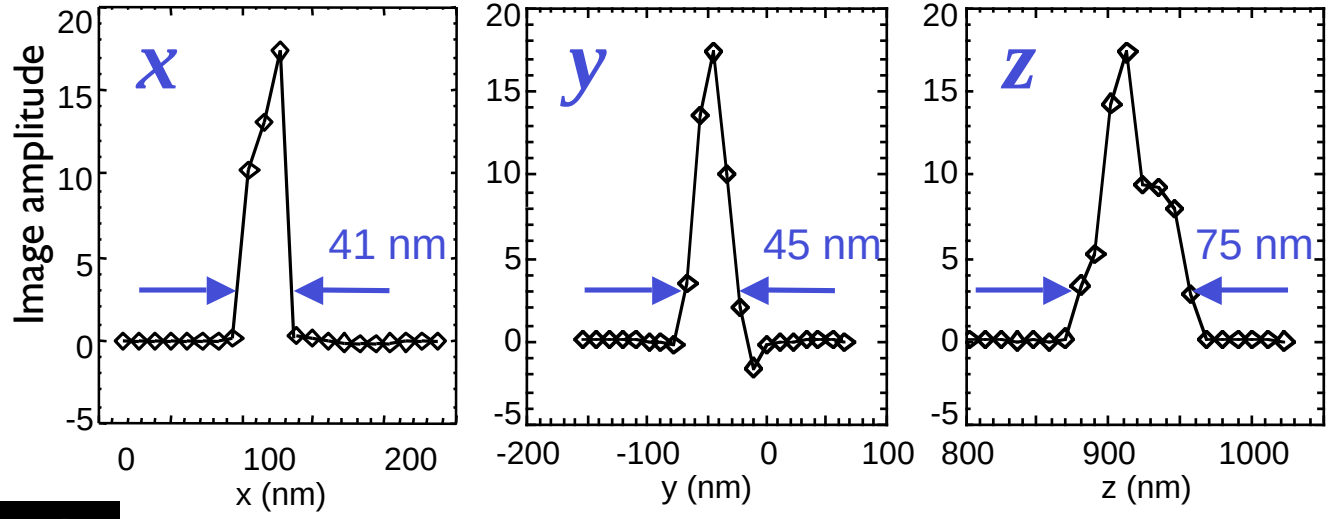

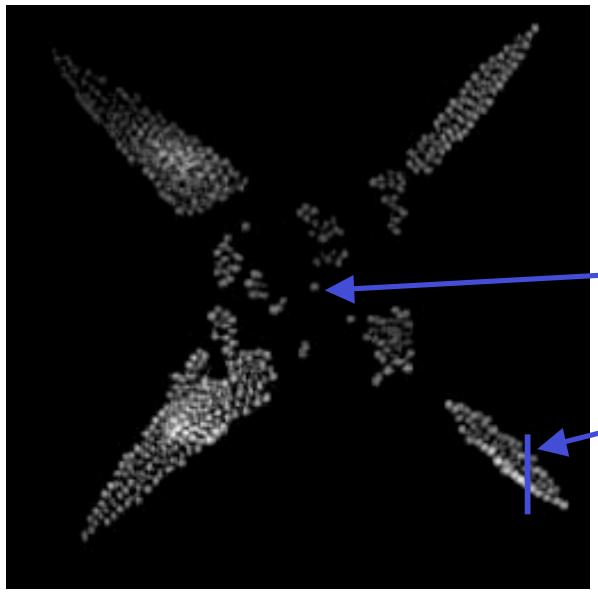

One 50 nm ball

Three50 nm balls

Line-outs of three balls in a row

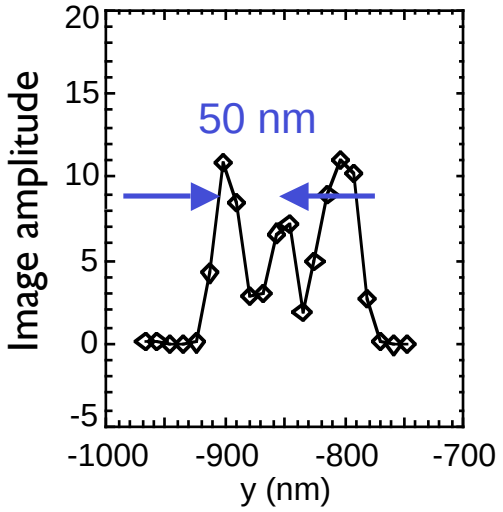

Slide courtesy H. Chapman LLNL

THE CONSISTENCY OF THE RECONSTRUCTED PHASES CAN BE QUANTIFIED

Is the solution unique? Can we determine a confidence of the reconstructed phases?

According to Veit Elser (Cornell) the answer is average the complex amplitudes of many reconstructions with different random starts, then compare $|\langle F \rangle|^2$ to measured intensity. If phase recovery of particular pixels is unsuccessful they will return random results and will average to near zero. If recovery of is good they will return consistent results similar to $|\langle F \rangle|^2$

We define an "algorithm transfer function" for 2D projection by averaging random starts

$$\frac{\left|\langle F(q)\rangle\right|^2}{I(q)} = \langle \cos\varphi \rangle^2$$

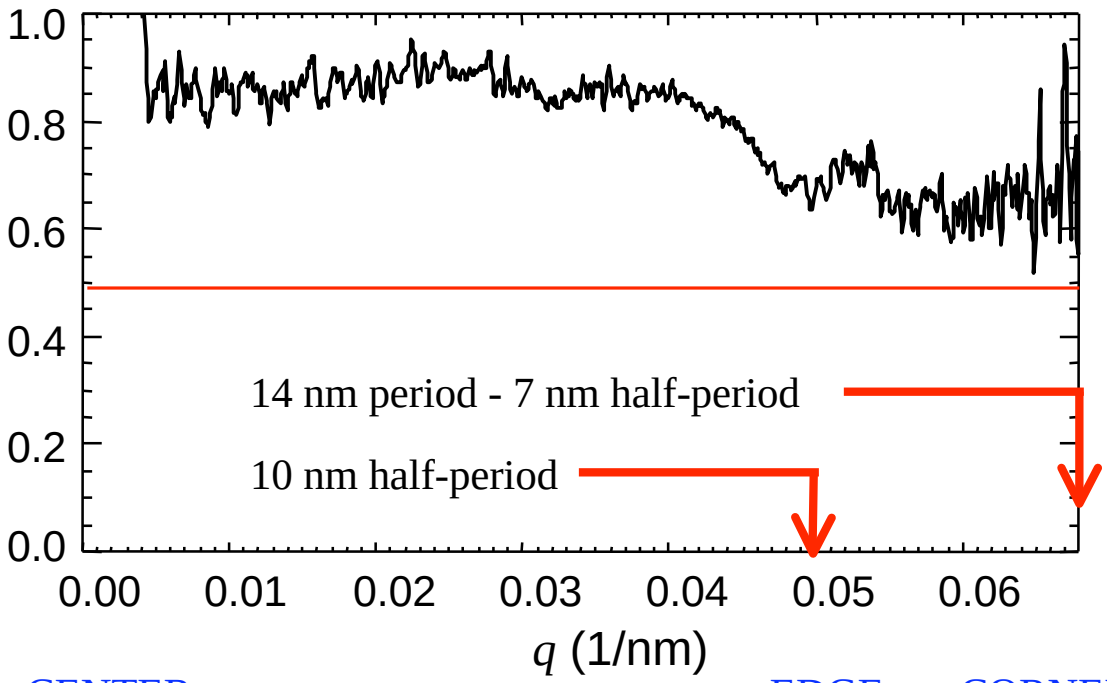

Slide: courtesy S. Marchesini, LBNL

3D IMAGE RECONSTRUCTIONS FROM EXPERIMENTAL X-RAY DATA (by Anton Barty of LLNL)

Voxel Data cube 1024^3 elements

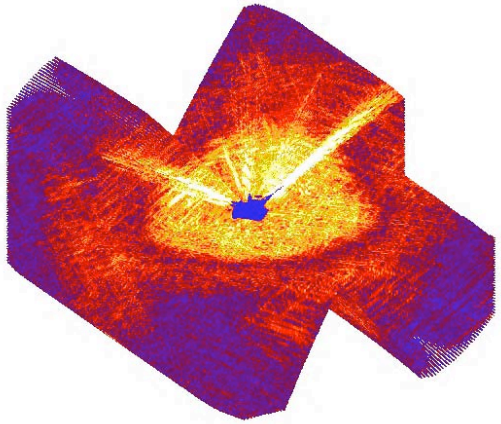

Iterative reconstruction algorithm
a few 1000s of 3D FFTs required

Reconstruction

Size	Memory needed	
	Single Precision	Double Precision
256^3	336 MB	592 MB
512^3	2.6 GB	4.7 Gb
1024^3	22 GB	38 GB
2048^3	176 GB	304 GB

Size	32-CPU G5 cluster speed	
	3D FFT timing	Processing time*
256^3	73 msec	10 mins
512^3	850 msec	1.5 hrs
1024^3	8 sec	14 hrs
2048^3	??	??

*2000 iterations, 2FFTs per iteration plus other floating point operations

code: C with mvapich, dist_fft (Altivec-optimized MPI FFT) see http://images.apple.com/acg/pdf/20040827_GigaFFT.pdf

Slide courtesy A. Barty LLNL

INVESTIGATION OF A 2μm AEROGEL STRUCTURE

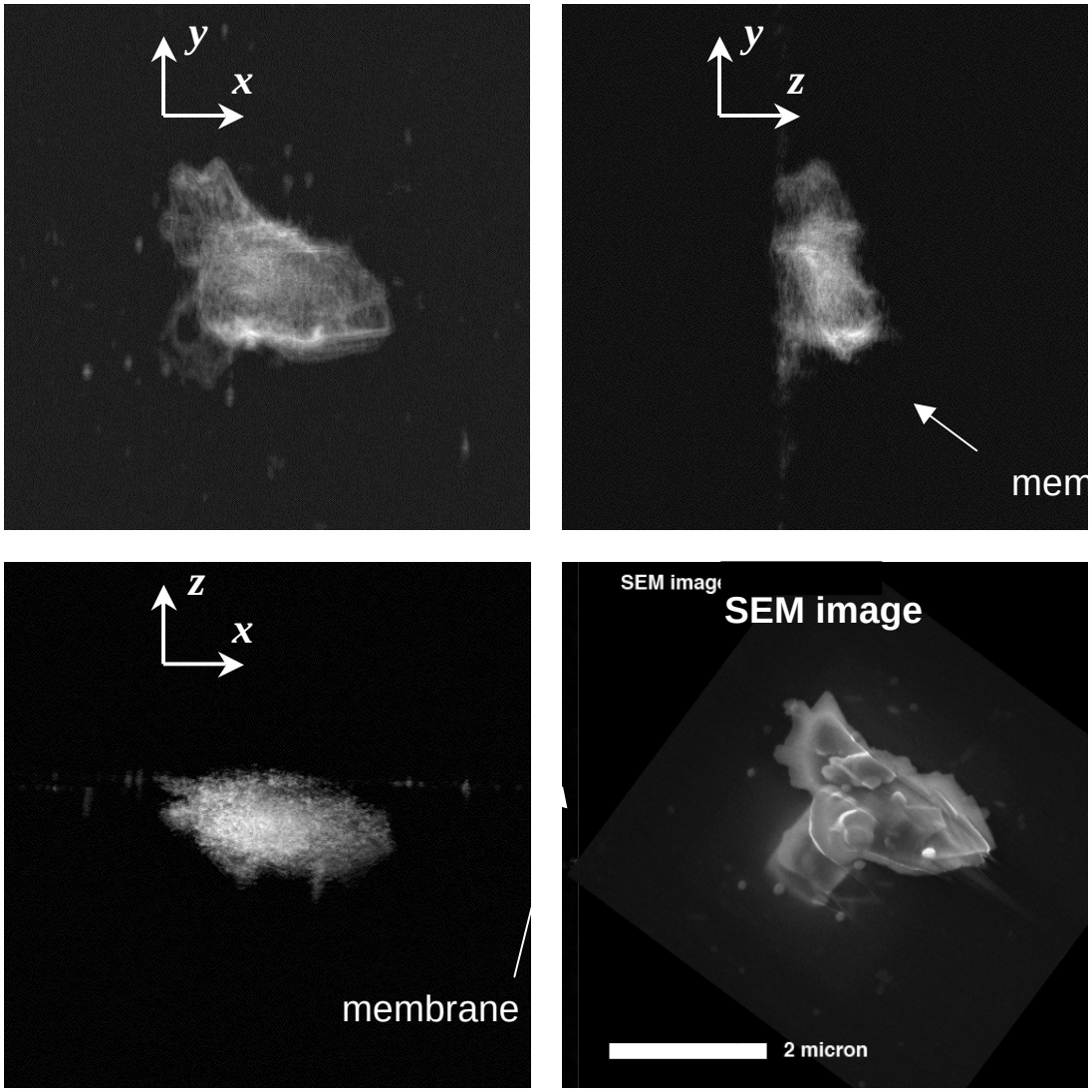

- [Barty et al PRL 2008 (in press), preprint - http://arxiv.org/abs/0708.4035v1]
- Ta_2O_5 aerogel (0.1 gm/cm^3), (bulk density = 8.5 gm/cm^3)
- Reconstructed images along orthogonal views
- Reconstruction details: 3D HIO with $\beta = 0.9$ for 300 iterations with support refinement followed by RAAR (relaxed averaged alternating reflections) algorithm [D. R. Luke 2005] (also with $\beta = 0.9$) through to iteration 2000

Slide: A. Barty, LBNL

3D AEROGEL RECONSTRUCTION
(by A. Barty LLNL)

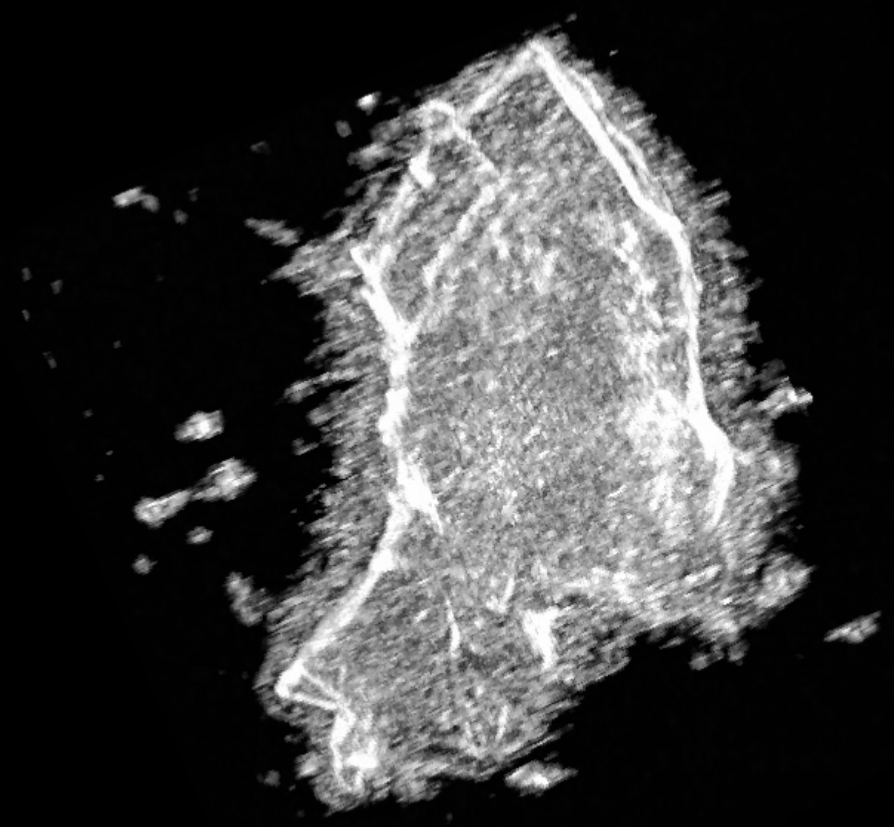

1 micron

THE 3D AEROGEL IMAGES REVEAL ITS SKELETON STRUCTURE

Mechanical analysis: J.Kinney (LLNL)

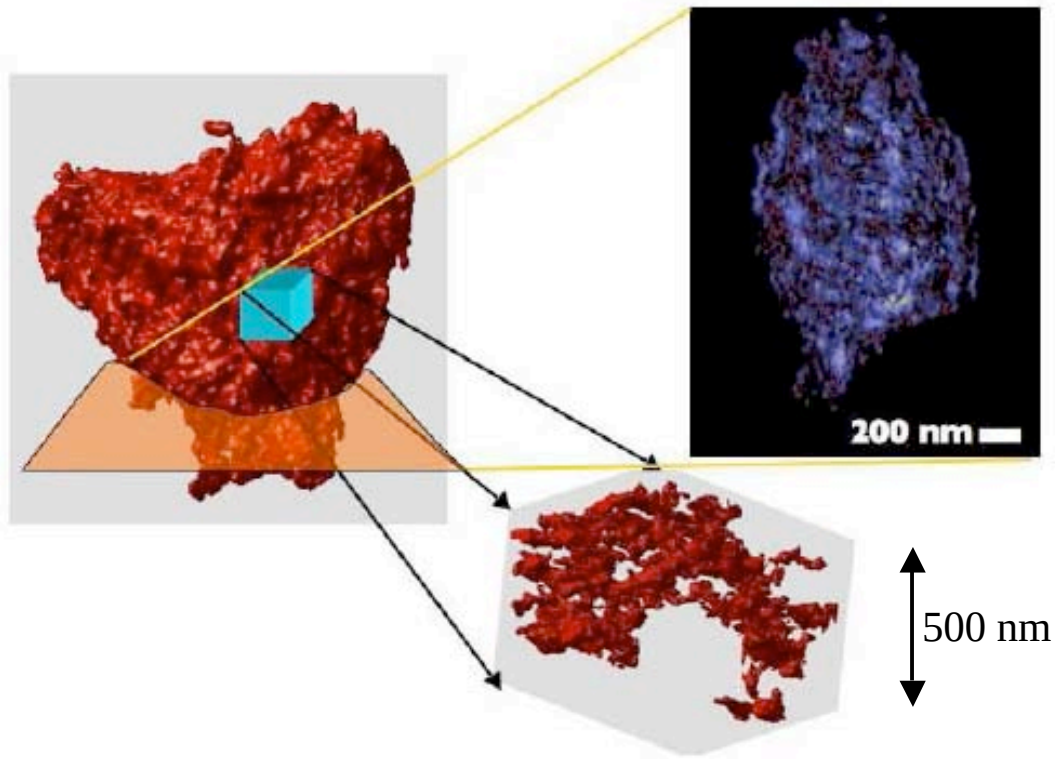

Section and isosurface rendering of a 500 nm cube from the interior of the 3D volume. The foam structure shows globular nodes that are interconnected by thin beam-like struts. Approximately 85% of the total mass is associated with the nodes, and there is no evidence of a significant fraction of dangling fragments.

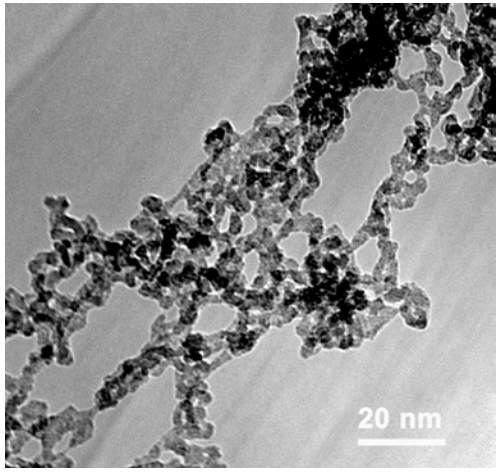

Electron microscope examination of a thin portion near a sample edge - only a few these can be found thin enough

COMPARISON OF AEROGEL RESULTS WITH USAXS-MEASURED DATA

[Barty et al PRL 2008 (in press)]

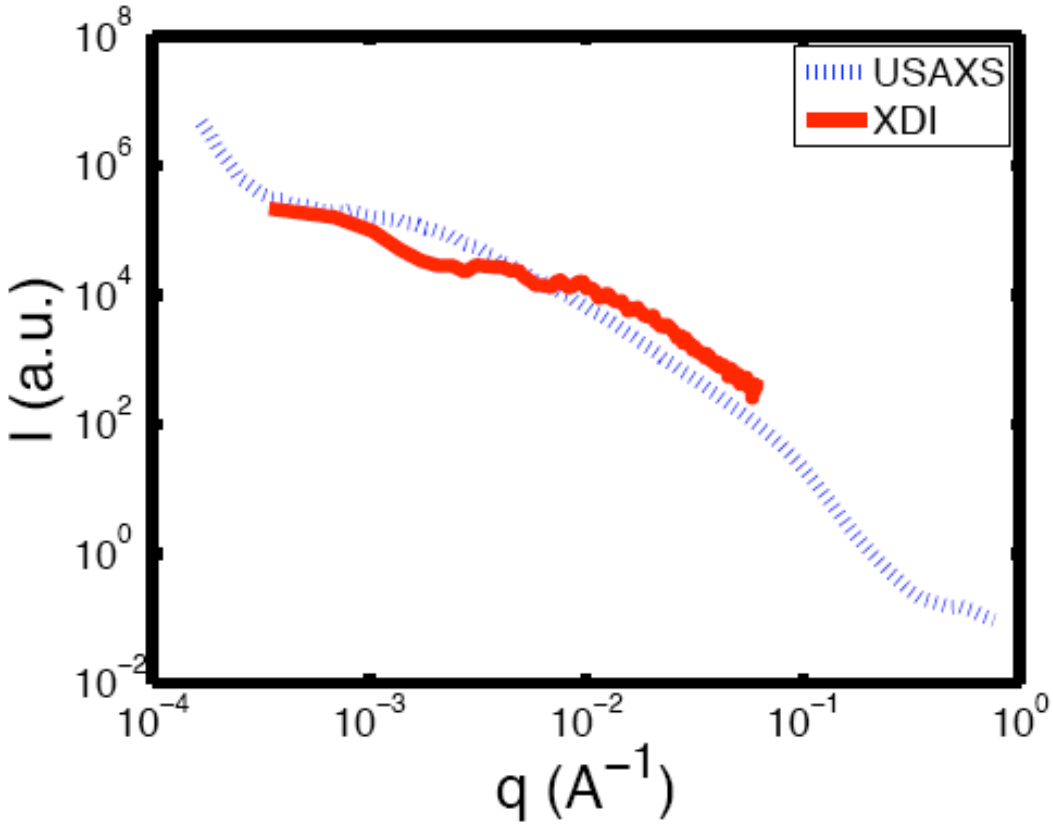

Small angle x-ray scattering data calculated from the 3D volume reconstruction (XDI) compared to ultra small angle x-ray scattering (USAXS) measurements [Ilavski et al 2002, 2004 (SRI)] on a similar batch of 100 mg/cc Ta_2O_5 aerogel

PROJECTED RESOLUTION AND EXPOSURE TIME FOR A NEW BEAM LINE (ALS "COSMIC" PROJECT)

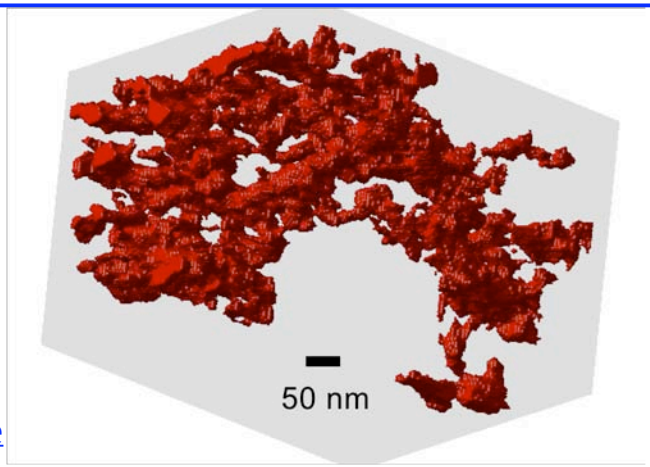

Aerogel sample: Estimate of resolution by the algorithm transfer function is 10 nm

Present beam line

- 280 views ±70° at 0.5° intervals - resolution 10 nm - sample density = 0.1 gm/cc
- Total time taken - 24 hours of which 8 hours is set-up, 8 hours exposing, 8 hrs overhead tasks

COSMIC beam line: superior flux on sample to present one by:

- Factor 15 due to ALS upgrade and optimised undulator brightness
- Factor 5 due to getting stigmatic BL optics (this has recently been done)
- Factor 6 due to improved component efficiencies - pinhole especially
- Overall factor 450
- Assume we are no longer limited by detector readout
- We project $10/\sqrt[4]{450} = 2.1$ nm resolution in 8 hours or 10 nm in a 1 minute exposure
- This improvement of resolution means 450 time more dose!!!

THE DOSE FRACTIONATION THEOREM OF STANDARD TOMOGRAPHY

R. Hegerl and W. Hoppe, Zeitschrift Naturforsch **3a**, 1717-1721 (1976), Abstract:

- "A three-dimensional reconstruction requires the same integral dose as a conventional two-dimensional micrograph provided that the level of (statistical) significance and the resolution are identical. The necessary dose D for one of the K projections in a reconstruction series is, therefore, the integral dose divided by K"
- The discussion provided by the originators of the theorem was largely in terms of a single voxel but, as pointed out by McEwan et al 1995, the conclusion can be immediately generalized to a full 3D object by recognizing that conventional tomographic projections are *linear* superpositions of the contributions of the individual voxels. A similar argument in frequency space shows that the theorem also applies to CXDI.
- Study by B. McEwan, K. Downing, R. Glaeser Ultramicroscopy **60**, 357-373 (1995) extended the validity to cases with:
  - high absorption
  - signal-dependent noise
  - varying sample contrast
  - missing angular range
  - a need to align the recorded patterns by cross-correlation methods

CALCULATION OF THE DOSE AND FLUX REQUIRED FOR TOMOGRAPHIC IMAGING WITH A GIVEN RESOLUTION

[Howells JESRP, 2008 (in press)] - preprint - http://arxiv.org/abs/physics/0502059

- Calculation based on dose fractionation theorem (previous slide)
- The coherent scattering cross section of a cubic voxel is $r_e^2 \lambda^2 |\rho|^2 d^4$ Note that the differential and total (Thomson) cross sections are both independent of wavelength. This cross section is an integral of the differential cross section between angular limits that are determined by a resolution requirement. It therefore gets a wavelength dependence from those limits
- The dose D and the flux F required to deliver P scattered x-rays into a detector with collection angle chosen for resolution d is

$$D = \frac{\mu P h\nu}{\varepsilon} \frac{1}{r_e^2 \lambda^2 |\rho|^2 d^4} \qquad F = \frac{P}{r_e^2 \lambda^2 |\rho|^2 d^4}$$

μ = the voxel intensity absorption coefficient
$h\nu$ = the photon energy
r_e = the classical electron radius
λ = the photon wave length
ρ = the voxel electron density
ε = the density

The dose scales as the inverse fourth power of the resolution

MEASUREMENT OF THE POWER LAW

- Record diffraction patterns with a wide range of exposure times 1-512s
- Fit polynomial to power spectrum
- Determine limiting spatial frequency where scattered power drops to noise
- Plot limiting spatial frequency versus single shot exposure time

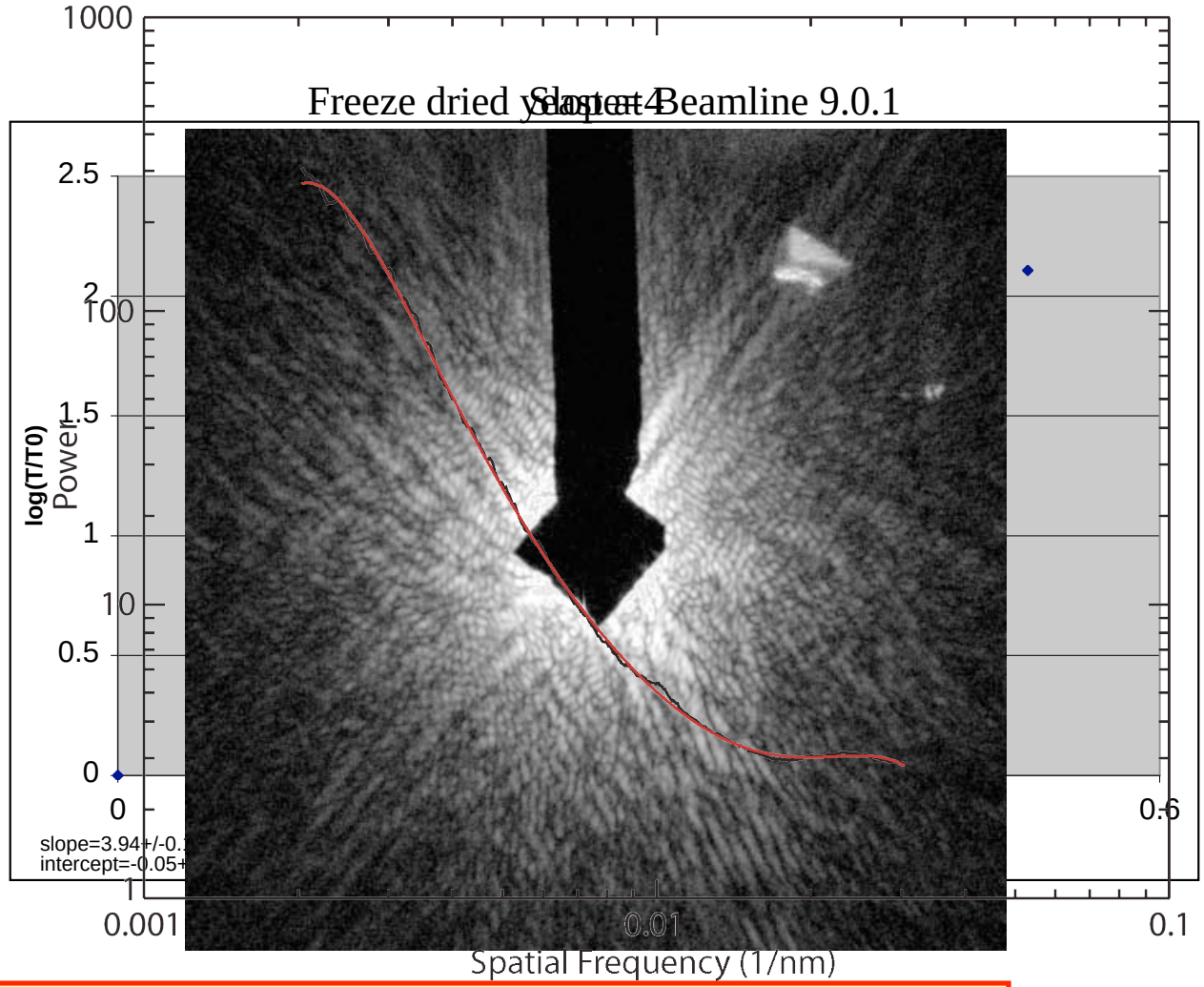

Slide courtesy D. Shapiro

Exposure time scales as the fourth power of the spatial frequency

FLUX REQUIREMENTS

Flux to detect a 10 nm voxel made of protein according to the Rose criterion.
A detector collecting an angle chosen for 10 nm resolution is assumed

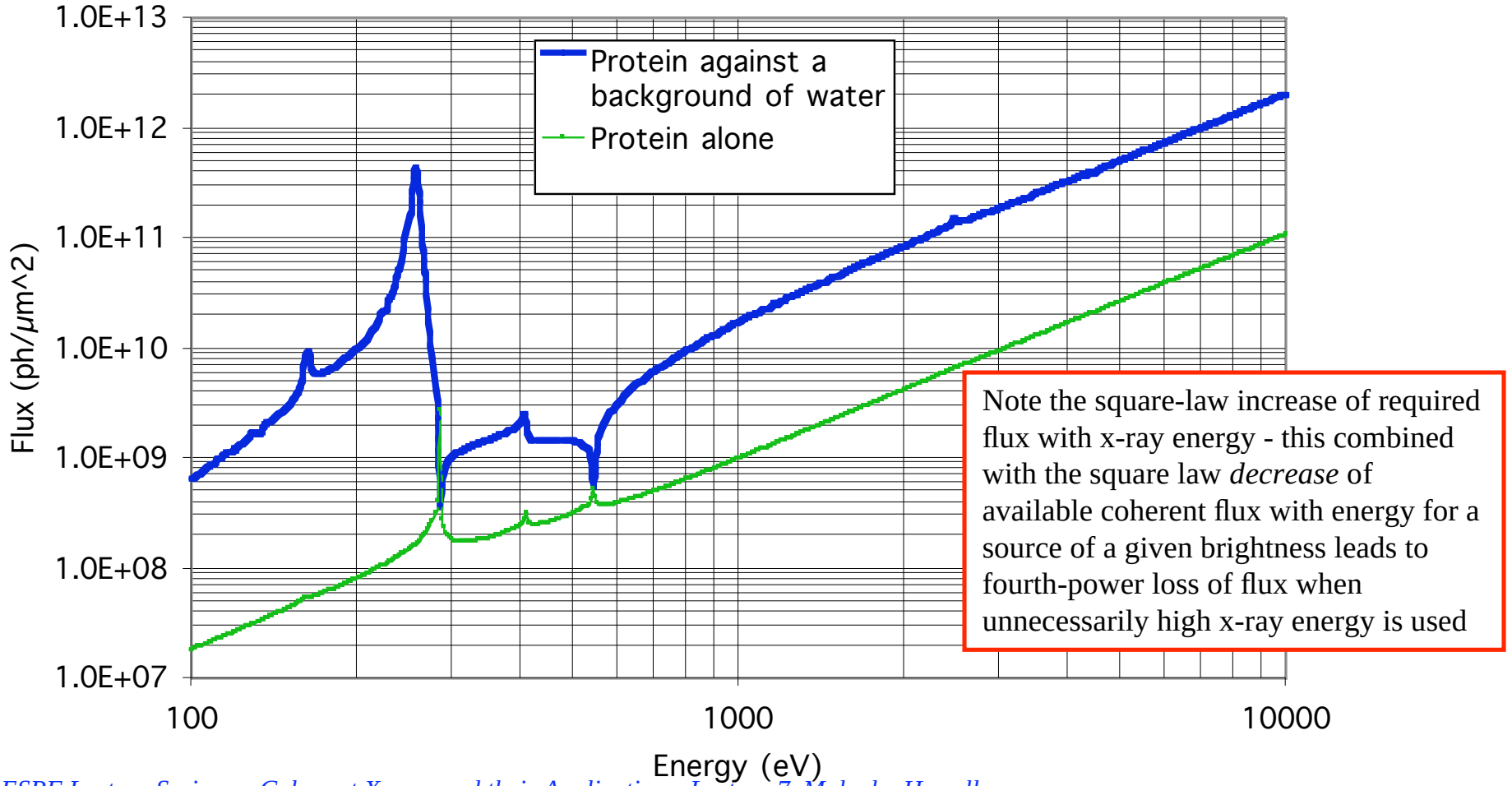

Note the square-law increase of required flux with x-ray energy - this combined with the square law *decrease* of available coherent flux with energy for a source of a given brightness leads to fourth-power loss of flux when unnecessarily high x-ray energy is used

DOSE REQUIREMENTS

Below is the dose to detect a 10 nm voxel made of protein according to the Rose criterion. A detector collecting an angle chosen for 10 nm resolution is assumed

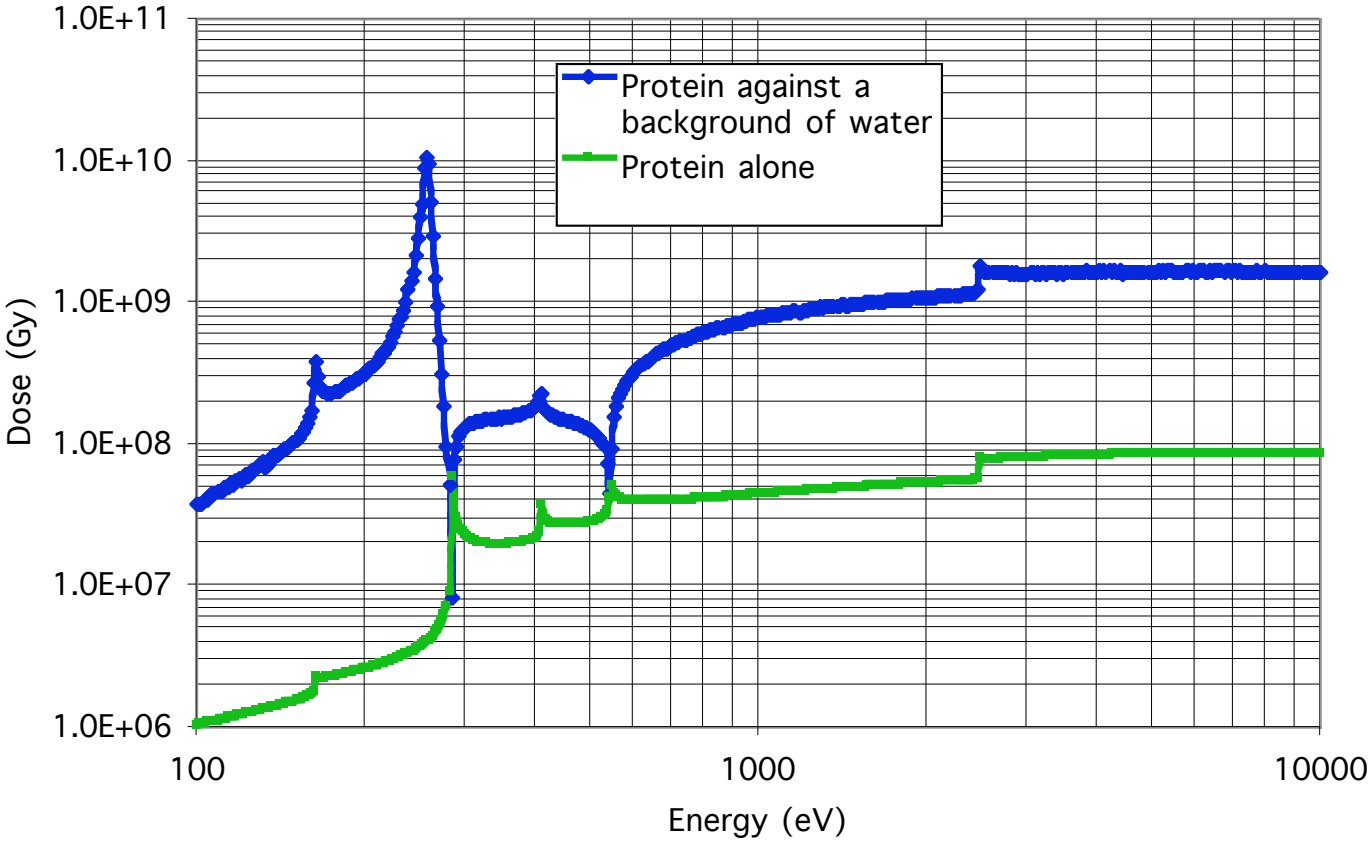

DIFFRACTION SPOT-FADING EXPERIMENT ON ALS BEAM LINE 8.3.1 (J. HOLTON)

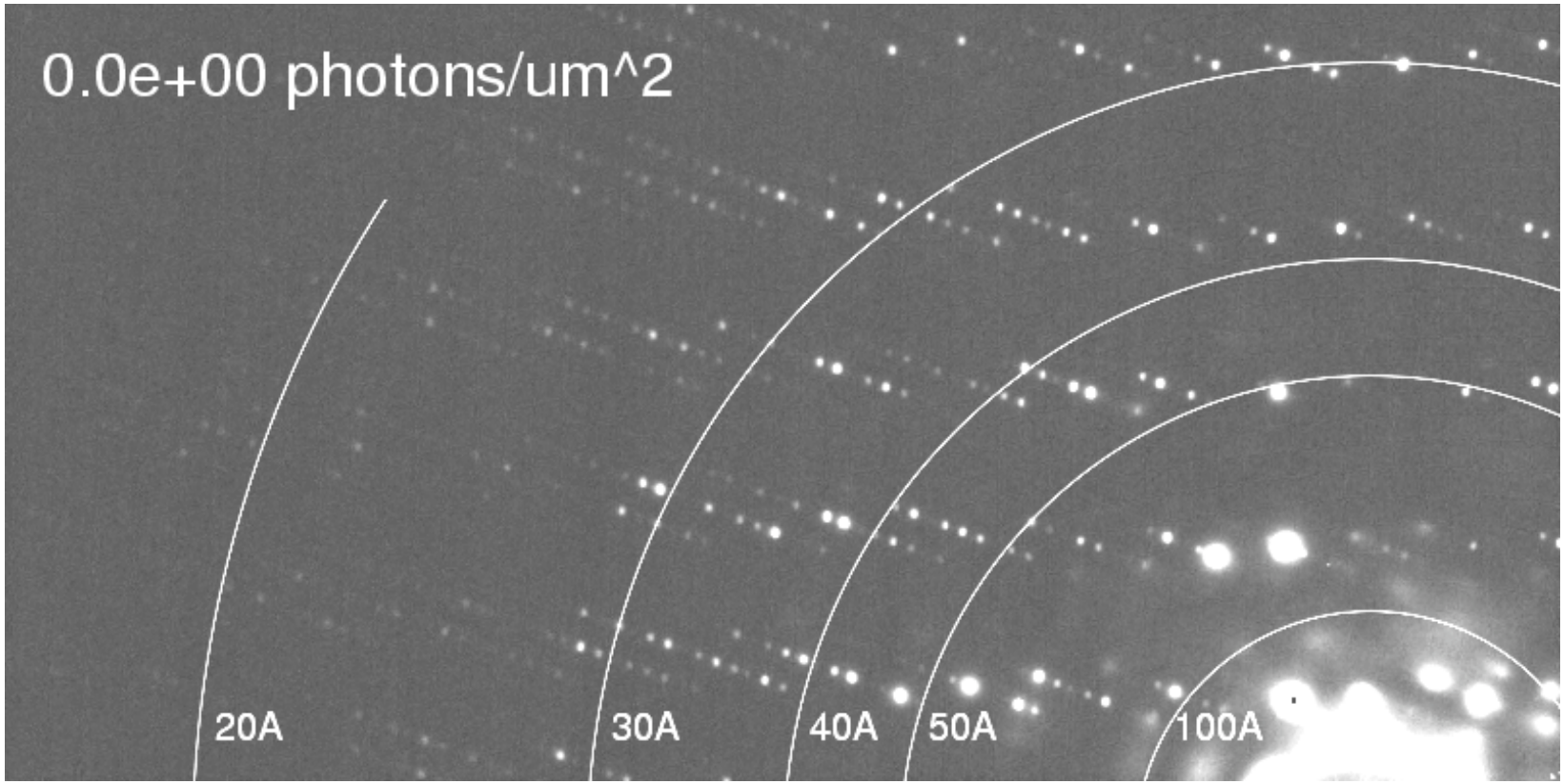

- Ribosome crystals (J. Cate) [Howells et al JESRP 2008 in press]
- About 24 hour exposure at 10 keV
- Long "dosing" exposures with slits wide were alternated with shorter "measurement" exposures with slits narrow

DOSE-RESOLUTION RELATIONSHIP FOR 3D IMAGING OF FROZEN-HYDRATED SAMPLES

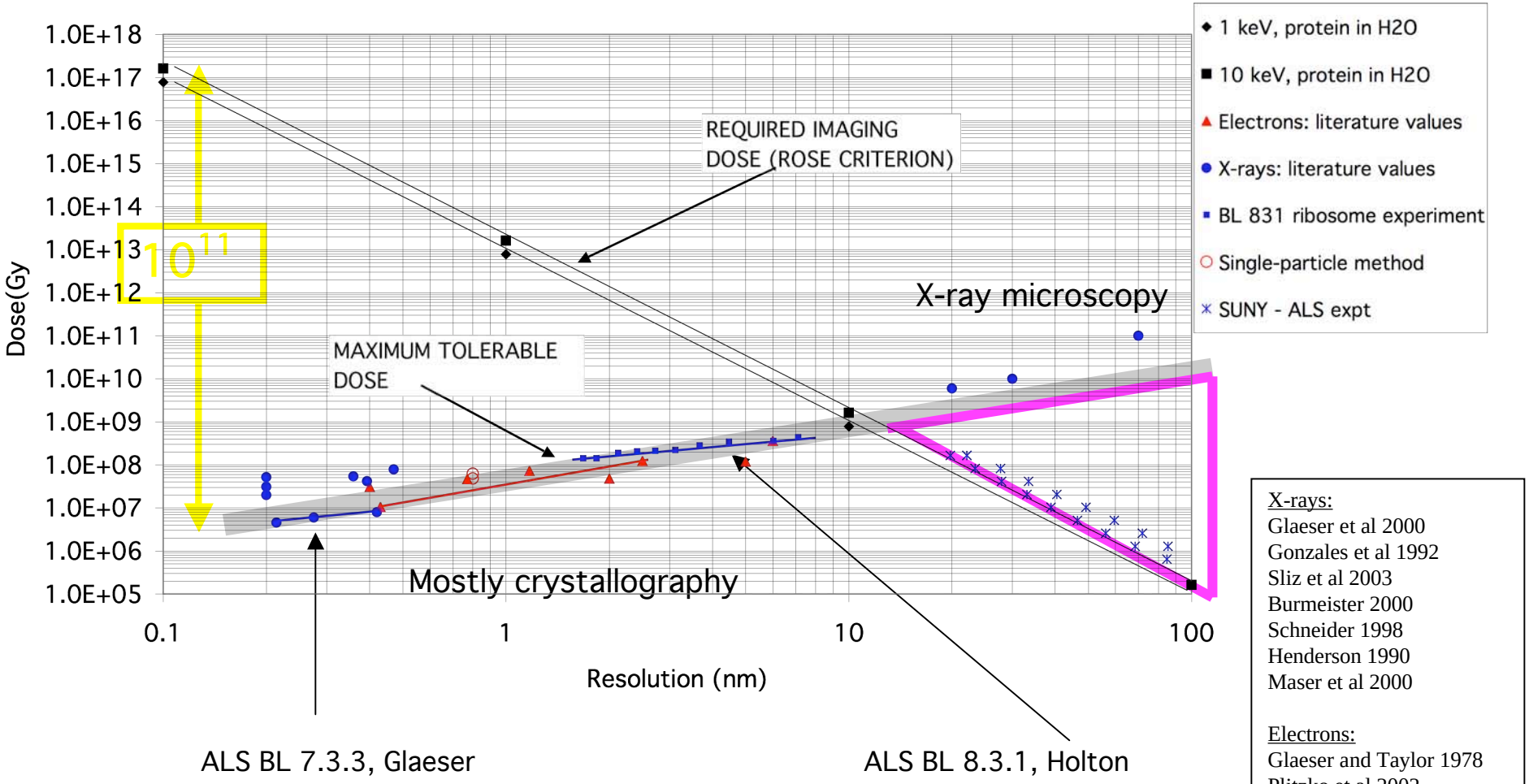

X-rays:
Glaeser et al 2000
Gonzales et al 1992
Sliz et al 2003
Burmeister 2000
Schneider 1998
Henderson 1990
Maser et al 2000

Electrons:
Glaeser and Taylor 1978
Plitzko et al 2002
Hayward and Glaeser 1979

SUMMARY AND CONCLUSIONS ON DOSE AND DAMAGE

Summary of conclusions from the graph on the last slide

- This calculation applies to diffraction by natural (unlabelled) protein against a background of water.
- Diffraction imaging experiments are only possible in the pink triangle to the right.
- According to the Rose criterion the dose-limited resolution by CXDI under the given conditions is predicted to be 10 nm.
- The quoted electron and x-ray results for the maximum tolerable dose agree well as we believe they should.
- The fourth-power dependence of dose on resolution is obtained by both calculation and experiment - straightness of the dose resolution plot for a particular sample offers a possible test for the onset of damage.
- The dose is expected to have only a weak dependence on x-ray energy.
- The calculation predicts what is already generally believed - that at least 10^{11} copies of the sample are required to solve a structure crystallographically to atomic resolution.
- Possible strategies for overcoming the 10-nm limit include (i) the use of labelling to improve the contrast and thus the resolution for a given tolerable dose and (ii) the use of samples with more order (prior knowledge) than a cell of completely unknown structure, for example fibers.

CALCULATION OF EXPOSURE TIME FOR A 2D IMAGE WITH ROSE-CRITERION IMAGE QUALITY FOR COHERENT X-RAY DIFFRACTION MICROSCOPY

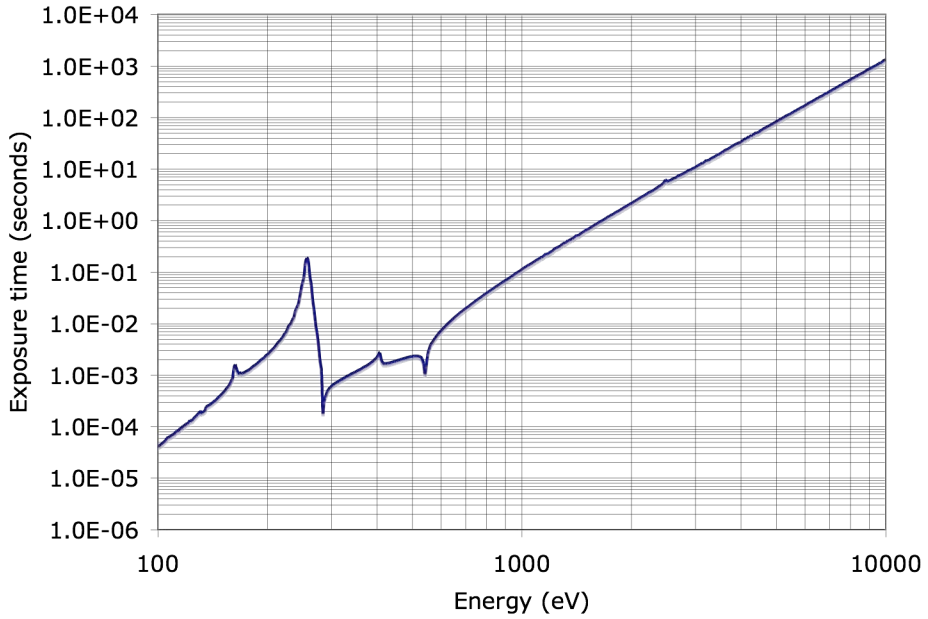

Using coherent flux $= B\left(\lambda/2\right)^2$

and fractional BW=1/(N/2), we get

$$T = \frac{2PA}{r_e^2 \lambda^4 \left|\rho_{eff}\right|^2 d^4 KB}$$

B is the brightness in usual units, K is the detector resolution in reciprocal kilopixels eg a 4000 pixel detector has K=0.25 - K determines the BW, A is the sample area

ASSUMPTIONS:

- Lossless beam line
- A coherent (single-mode) beam is exactly delivered to fill the sample area
- Number of scattered x-rays per pixel P = 25 (Rose criterion)
- Parameter values: A=10x10μm^2, $|\rho_{eff}|^2$ is for protein against a background of water, d=10 nm, K=1 (1000x1000 detector) and B=10^{19} usual units
- Note that for a given source brightness the exposure time increases roughly as (energy)^4